FINAL REPORT

Estimated Exposure and Lifetime Cancer Incidence Risk from Routine Plutonium Releases at the Rocky Flats Plant

Part of Task 3: Independent Analysis of Exposure, Dose, and Health Risk to Offsite Individuals

Revision 1
August 1999

Submitted to the Colorado Department of Public Health and Environment, Disease Control and Environmental Epidemiology Division, Rocky Flats Health Studies in partial fulfillment of Contract No. 100APPRCODE 391

Radiological Assessments Corporation
417 Till Road Neeses, South Carolina 29107
phone 803.536.4883 fax 803.534.1995

FINAL REPORT

Estimated Exposure and Lifetime Cancer Incidence Risk from Routine Plutonium Releases at the Rocky Flats Plant

Part of Task 3: Independent Analysis of Exposure, Dose, and Health Risk to Offsite Individuals

Revision 1
August 1999

Author

Arthur S. Rood, K-Spar, Inc.

Principal Investigator

John E Till, Ph.D., *Radiological Assessments Corporation*

EXECUTIVE SUMMARY

The Rocky Flats Environmental Technology Site is owned by the U.S. Department of Energy (DOE) and is currently contractor-operated by Kaiser-Hill Company. For most of its history, the site was called the Rocky Flats Plant (RFP) and was operated by Dow Chemical Company as a nuclear weapons research, development, and production complex. The RFP is located about 8–10 km (5–6 mi) from the cities of Arvada, Westminster, and Broomfield, Colorado and 26 km (16 mi) northwest of downtown Denver, Colorado.

Through a 1989 Agreement in Principle between the DOE and the State of Colorado, DOE provided the State with funding and technical support for health-related studies. The purpose of the Historical Public Exposures Studies on Rocky Flats is to identify potential health effects in residents in nearby communities who may have been exposed to past toxic and radioactive releases.

This report documents risk calculations for inhalation of plutonium[a] in air resulting from routine operational releases at the RFP during 1953–1989. The report summarizes the routine operational release estimates for plutonium reported in Voillequé (1999) that provide the source term for these risk calculations. The historical environmental monitoring data that may be useful for validating the models used to calculate the risks are evaluated, and the environmental transport modeling procedure and results are described. Estimates of airborne concentrations of plutonium with uncertainty are provided along with lifetime carcinogenic incidence risk resulting from inhalation of plutonium for generic receptor scenarios.

Source Term. Estimated annual routine operational plutonium releases with uncertainty were investigated and documented in Voillequé (1999) and used without modification. Routine emissions exclude the episodic releases that resulted from the 1957 and 1969 fires, and the wind-driven suspension of contaminated soils from the 903 Area. Routine operational releases occurred from the 44-m stack of Building 771 and from roof vents on Building 776/777. Effluent was passed through HEPA filtration resulting in particle sizes generally less than 1 μm being released. Median annual release estimates ranged from about 0.06 μCi in 1989 to 3×10^4 μCi in 1957.

Environmental Monitoring. Historical environmental monitoring data that are pertinent to routine releases of plutonium and that may be useful for validation efforts are reviewed. This would include the source term estimates and the environmental transport models. Monitoring of plutonium in air, water, and soil has been conducted at the site since the start of operations. These data were evaluated in Rope et al. (1999). In general, air monitoring data was of little use prior to 1970 because of a variety of reasons, including, only gross alpha was measured, poor detection limits, and other more significant sources tended to obscure impacts seen from routine operations. Comparison of model predictions with post 1970 air monitoring was also complicated by the presence of other sources of RFP plutonium, in particular, suspension of plutonium contaminated soil from the field east of the 903 Area. Plutonium deposition was also monitored with gummed paper collectors, however, interpretation of the results was complicated by poor detection limits and the presence of other sources of environmental plutonium. For these reasons,

[a] In this context, the word plutonium means weapons grade plutonium, which consists primarily of ^{239}Pu (93.8%), ^{240}Pu (5.8%), and ^{241}Pu (0.36%) by weight percent. Specific activity of weapons grade plutonium is 0.072 Ci g^{-1}.

comparison of model predictions with environmental monitoring data was documented in a separate report (Rood and Grogan 1999) that considers all sources of airborne plutonium.

Environmental Transport Modeling. Five atmospheric transport models ranging from a simple straight-line Gaussian plume model to a complex terrain model were evaluated for use in this study (Rood 1999). Models were compared to tracer measurements taken in the winter of 1991 at Rocky Flats. The results of this evaluation indicated no one model clearly outperformed the others. However, the puff trajectory models, RATCHET, TRIAD, and INPUFF2 generally had lower variability and higher correlation to observed values compared to the other models. The RATCHET model was chosen for these calculations because it was particularly well suited for long-term annual-average dispersion estimates and it incorporates spatially varying meteorological and environmental parameters.

The model domain encompassed a 2,200 km^2 area (50 km north-south by 44 km east-west). The domain extended 28 km south, 12 km west, 22 km north, and 32 km east from the RFP. Most of the Denver metropolitan area and the city of Boulder were included in the domain. Reliable meteorological data from RFP is lacking before 1984. For this reason, a recent 5-year (1989–94) meteorological data set was used to determine annual average X/Q (concentration divided by release rate) values for 2300 receptor locations in the model domain. Meteorological data taken at the Denver Stapleton International Airport during the same period was also incorporated into the simulations. Annual average concentrations for each year were then determined by multiplying the annual release rate by the appropriate X/Q value.

Treatment of Uncertainty. Risk estimates were reported as probability distributions that reflect our current state of knowledge of the problem. They do not represent the probability of a seeing a health effect within the population of potential receptors. Model prediction uncertainty was accounted for through the use of several multiplicative stochastic correction factors that accounted for uncertainty in the dispersion estimate, the meteorology, and deposition and plume depletion. Dispersion uncertainty was based on distributions on predicted-to-observed ratios from field tracer experiments using the Gaussian plume and other models including RATCHET. These values were derived from literature reviews and results from studies specific to this project. Meteorological uncertainty arises because we are using 5 years of meteorological data spanning a recent time period (1989–1993) to define an annual average X/Q value that will be applied to all previous years of the assessment period (1953–1989). This correction factor was derived from studies performed for the Fernald Dosimetry Reconstruction Project (Killough et al. 1998) and additional comparisons made at Rocky Flats. Deposition and plume depletion uncertainty factors were calculated using the Monte Carlo sampling features of RATCHET. All correction factors were distributed lognormally and were combined with the source term uncertainty to yield distributions of predicted concentrations at selected receptor locations. Monte Carlo techniques were used to propagate model prediction uncertainty through to the final risk calculations.

Predicted Concentrations. Median value predicted concentrations of plutonium east of the plant along Indiana Avenue ranged from 0.1 fCi m^{-3} in 1957 to 5×10^{-5} fCi m^{-3} in 1978. This can be compared to weapons testing fallout concentrations of 0.1 fCi m^{-3} in 1957 and 4×10^{-2} fCi m^{-3} in 1978. The geometric standard deviation of model predicted concentrations was typically around 2 to 2.4.

Exposure Scenarios. Inhalation was the only pathway considered in the evaluation. This decision was based on the Phase 1 results (ChemRisk 1994c) that showed soil ingestion and

inhalation of resuspended plutonium to be minor pathways when considering the long-term exposure to Rocky Flats effluent. The risk that a person receives depends upon a number of factors, such as

- Where a person lived and worked in relation to the RFP.
- When and how long that person lived near the RFP
- Age and gender of the person
- Lifestyle (that is, did the person spend a great deal of time outdoors or doing heavy manual work)

To consider these features of a person's life, we developed profiles, or exposure scenarios, of hypothetical, but realistic residents of the RFP area for which representative risk estimates could be made. Risks were calculated for nine hypothetical exposure scenarios. These scenarios incorporate typical lifestyles, ages, genders, and lengths of time in the area. and can help individuals determine risk ranges for themselves by finding a lifestyle profile that most closely matches their background. The scenarios provide a range of potential profiles of people in the area.

The nine exposure scenarios include a rancher located outside the east cattle fence along Indiana Avenue, a housewife who lived in Broomfield, a child who grew up in Broomfield during the operational period of the RFP (1953–89), and several receptors (retiree and office worker) who moved into the Denver Metropolitan area in the 1970's. Each receptor scenario incorporates inhalation rates that reflect the individual's lifestyle. For example, the rancher's breathing rate reflects one who performs manual labor for part of the day. Uncertainty was not incorporated into the exposure scenarios; that is, the physical attributes and behavior of the receptors were fixed. The calculated risks were not intended to represent a population of receptors who exhibit a given behavior.

Plutonium Risk Coefficients. Lifetime cancer incidence risk coefficients (risk per unit intake) with uncertainty for ^{239,240}Pu inhalation were developed by Grogan et al. (1999) for four critical organs; lung, liver, bone surface and bone marrow. Where feasible, sex and age specific risk coefficients were determined.

Risk Estimates. Geometric mean incremental lifetime cancer incidence risk estimates for plutonium inhalation were greatest for the lung followed by the liver, bone surface, and bone marrow. The rancher scenario exhibited the highest risks. Total risks (the sum of all four organs) for the rancher ranged from 1.0×10^{-8} (5% value) to 2.1×10^{-6} (95% value). Using the rancher scenario as an example, these risks may be interpreted as follows:

- *There is a 90% probability that incremental lifetime carcinogenic incidence risk to the lung for the rancher was between 1.0×10^{-8} (5% value) and 2.1×10^{-6} (95% value).*
- *There is a 5% probability that incremental lifetime carcinogenic incidence risk to the lung for the rancher was greater than 2.1×10^{-6}. and a 5% probability the risk was less than 1.0×10^{-8}.*

Risk estimates were within the EPA point of departure for acceptable risks (10^{-6} to 10^{-4}).

CONTENTS

FIGURES

TABLES

ACRONYMS

AMAD	activity median aerodynamic diameter
CDPHE	Colorado Department of Public Health and Environment
CV	coefficient of variation
DOE	U.S. Department of Energy
EPA	U.S. Environmental Protection Agency
GM	geometric mean
GSD	geometric standard deviation
HAP	Health Advisory Panel
HASL	Health and Safety Laboratory of the Atomic Energy Commission
INPUFF2	INtegrated PUFF dispersion code version 2.0
ISC	Industrial Source Complex code
RAC	*Radiological Assessments Corporation*
RATCHET	Regional Atmospheric Transport Code for Hanford Emission Tracking
RFP	Rocky Flats Plant
TIC	time-integrated concentration
TLLa	total long-lived alpha activity
TRAC	Terrain Responsive Atmospheric Code
USGS	U.S. Geological Survey
UTM	universal transverse mercator

INTRODUCTION

The Rocky Flats Environmental Technology Site is owned by the U.S. Department of Energy (DOE) and is currently contractor-operated by Kaiser-Hill Company. For most of its history, the site was called the Rocky Flats Plant (RFP) and was operated by Dow Chemical Company as a nuclear weapons research, development, and production complex (Figure 1). The RFP is located on approximately 2,650 ha (6,500 acres) of Federal property, about 8–10 km (5–6 mi) from the cities of Arvada, Westminster, and Broomfield, Colorado and 26 km (16 mi). northwest of downtown Denver, Colorado. The original 156-ha (385-acre) main production area is surrounded by a 2,490-ha (6,150-acre) buffer zone that now delineates the RFP boundary.

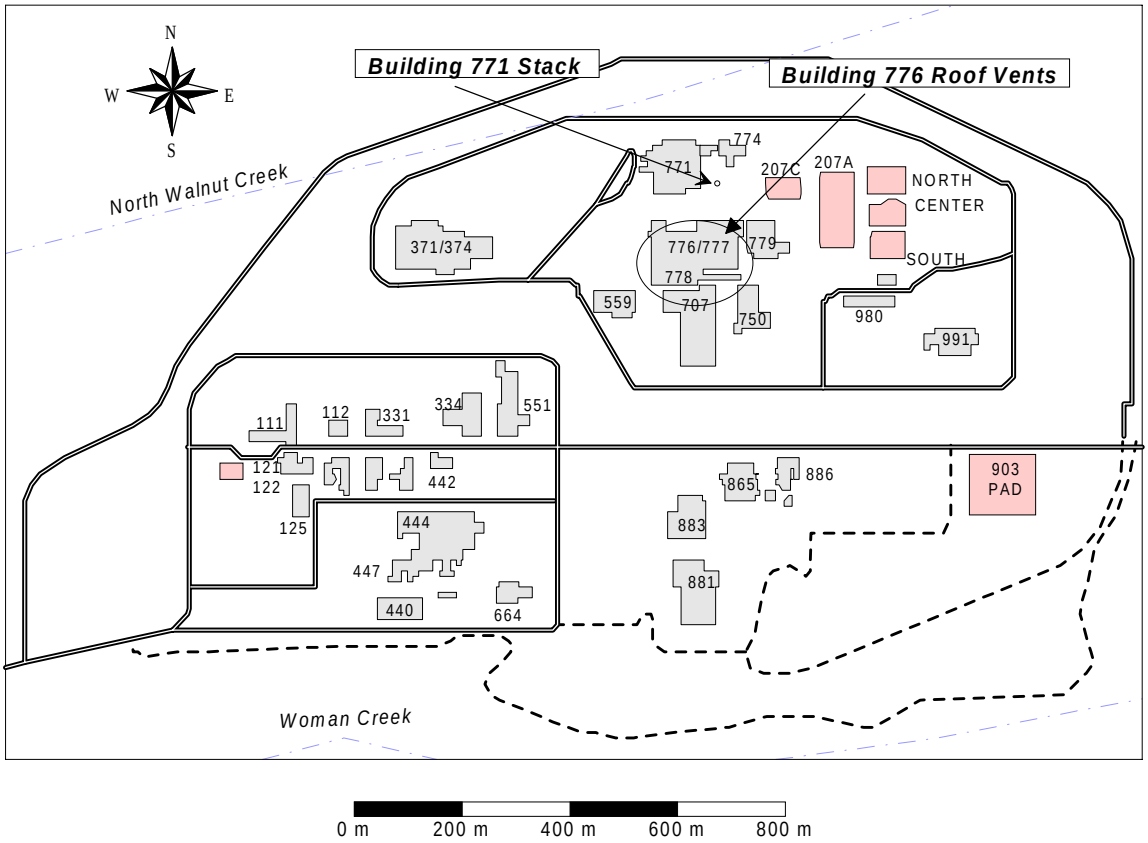

Figure 1. Main production area of the Rocky Flats Plant as it appeared in 1990. Originally, the buildings were identified with two-digit numbers. Later, a third digit was added. The production area, now sometimes called the industrial area, is surrounded by a security perimeter fence. The area between the perimeter fence and Indiana Street to the east is the buffer zone. The buffer zone was expanded to Indiana Street in the 1970s. Major plutonium release points (Building 771 stack and Building 776 roof vents) are identified.

Through a 1989 Agreement in Principle between the DOE and the State of Colorado, DOE provided the State with funding and technical support for health-related studies. The purpose of the Historical Public Exposures Studies on Rocky Flats is to identify potential health effects in residents in nearby communities who may have been exposed to past toxic and radioactive

releases. The Colorado Department of Public Health and Environment (CDPHE) first invited a national panel of experts to help design the health studies. Because of intense public concern about Rocky Flats contamination among Denver metropolitan area residents following a Federal Bureau of Investigation raid of Rocky Flats in June 1989, the panel decided to stress public involvement and to separate the research into two major phases conducted by two different contractors to enhance accountability and credibility.

Phase I of the study was performed by ChemRisk (a division of McLaren/Hart, Environmental Engineering). In Phase I, ChemRisk conducted an extensive investigation of past operations and releases from the RFP. The Phase I effort identified the primary materials of concern, release points and events, quantities released, transport pathways, and preliminary estimates of dose and risk to offsite individuals. The conclusions from Phase I were released in a public summary document (HAP 1993), a series of task reports by ChemRisk, and several articles in the journal *Health Physics*.

Radiological Assessments Corporation (*RAC*) was awarded the contract to conduct Phase II of the study, which is an in-depth investigation of the potential doses and risks to the public from historical releases from Rocky Flats. Recommendations for work to be performed in Phase II are outlined in the Phase I summary document HAP (1993).

This report documents lifetime cancer incidence risk calculations from inhalation of plutonium[a] in air originating from routine releases at the RFP. Routine emissions exclude the episodic releases that resulted from the 1957 and 1969 fires, and the meteorological conditions (primarily high winds) that led to suspension of contaminated soil from the 903 Area. Evaluation of risks is limited to the plutonium isotopes ^{239,240}Pu. Other alpha emitting nuclides were also present in the effluent (^{238}U, ^{241}Am); however, results from Phase I indicated plutonium was the dominant dose contributor. This report summarizes the Phase I results, the Phase II plutonium source term developed by Voillequé (1999). A detailed description of the environmental transport modeling used to estimate air concentrations and deposition in the model domain is provided. Soil, vegetation, and air monitoring data for plutonium are reviewed, but comparison with model predicted concentrations is not possible in this report because all significant plutonium sources need to be accounted for in the comparison. This is the subject of a separate report (Rood and Grogan 1999). The plutonium risk coefficients developed by Grogan et al. (1999) to determine the lifetime risk of lung cancer, liver cancer, bone cancer and leukemia (bone marrow exposure) per unit activity of ^{239,240}Pu inhaled are summarized. Lifetime cancer incidence risks are presented for nine generic receptor scenarios that are described in detail.

REVIEW OF THE PHASE I EVALUATION OF ROUTINE PLUTONIUM RELEASES

The Phase I evaluation of routine plutonium releases at the RFP is documented in the Task 5, 6, and 8 reports (ChemRisk 1994a, 1994b, 1994c). Routine emissions excluded the episodic releases that resulted from the 1957 and 1969 fires, and the suspension of contaminated soil from the 903 Area. Source term estimates are documented in the Task 5 report, environmental transport modeling and exposure scenarios are described in the Task 6 report, and radiation dose

[a] In this context, the word plutonium means weapons grade plutonium, which consists primarily of ^{239}Pu (93.8%), ^{240}Pu (5.8%), and ^{241}Pu (0.36%) by weight percent. Specific activity of weapons grade plutonium is 0.072 Ci g^{-1}.

and risk estimates are presented in the Task 8 report. Plutonium health effects in Phase I were reported in terms of effective dose equivalent and whole body cancer risk. The plutonium source term was based on compilations in the 1980 Final Environmental Impact Statement (DOE 1980). ChemRisk recalculated the annual release estimates for several years as a check, and in some cases modified the estimates to include smaller release incidents such as the 1965 glove-box drain fire and the 1974 control valve failure. Total plutonium release estimates from 1953 to 1989 were lognormally distributed and ranged from 17,927 μCi (5^{th} percentile) to 117,409 μCi (95^{th} percentile) with a 50^{th} percentile value of 46,081 μCi. The year of highest releases was 1957. All the plutonium was assumed to be released from Buildings 771 and 776.

Airborne transport of plutonium was performed using the Industrial Source Complex code (ISC) and 5-years of meteorological data taken at RFP from 1987 to 1991. Meteorological data for prior years of operation (1953–1986) were considered incomplete and of questionable integrity. Concentrations for unit releases (1 mCi) were calculated for receptors in a model domain that extended to Interstate 25 in the east, the city of Wheat Ridge in the south, the city of Boulder in the north, and the city of Eldorado Springs in the west. Plutonium concentrations in air and surface deposition for specific years were then scaled according to the estimated release for that year.

Exposure pathways included inhalation, ingestion, immersion, and ground shine. Ingestion pathways included consumption of soil, water, and contaminated food products (milk, meat, and produce). Inhalation pathways included direct inhalation and inhalation of contaminated soil resuspended from a contaminated ground surface. Air and ground surface concentrations were averaged across eight, 45-degree sectors at several distances away from the RFP. The receptor was assumed to reside in a given sector for a 1-year exposure period.

Radiological dose and estimates of excess lifetime cancer risk were calculated for each year during the operation of the plant and summed over a lifetime of exposure (1953–1989). Risk estimates included the risk of fatal and non-fatal cancer and severe hereditary effects. A risk conversion factor of 0.073 Sv^{-1} was used to convert effective dose equivalent (EDE) estimates to cancer risk estimates. For routine plutonium releases, the year of highest dose was 1957. Doses for that year ranged from 0.02 μSv (5^{th} percentile) to 0.45 μSv (95^{th} percentile) EDE (Figure 3-20 in ChemRisk 1994c). Highest doses were reported to occur in sectors south-southeast of the plant (reported as sector 12). Integrated dose over a lifetime of exposure (1953–1989) at the location of maximum dose ranged from 0.2 μSv (5^{th} percentile) to 0.7 μSv (95^{th} percentile) EDE (Figure 3-21 in ChemRisk 1994c). Cancer risk estimates were not reported for integrated exposure but can be calculated using the risk conversion factor of 0.073 Sv^{-1}. Using this factor, risk estimates for integrated lifetime exposure to plutonium released during routine operations ranged from 1.5×10^{-8} to 5.1×10^{-8}. The major exposure pathway was direct inhalation. Direct inhalation was typically an order of magnitude greater than the next highest exposure pathway. Soil ingestion becomes increasing more important during the later years of operation (1980–1989) because soil concentrations offsite are highest during the later years. However, total doses for these years were generally 1 to 2 orders of magnitude lower than the years of highest releases (1957–1970).

PHASE II PLUTONIUM SOURCE TERM ESTIMATES

Quantities of plutonium routinely released from the Building 771 stack and Building 776/777 roof vents are evaluated in Voillequé (1999). Historical release estimates were based on

effluent monitoring at a centerline location in the large exhaust ducts. The main issue examined was the effect of nonuniform concentration distributions in the large exhaust ducts. Calculation of annual releases addressed the problems of nonrepresentative sampling and incorporated the estimates of bias developed in Phase I. Empirical relationships between the centerline air concentration and values at two other locations in the duct were developed for individual sampling periods. Those data were used together with knowledge of the duct arrangement and professional judgment to develop the relationships that permitted estimation of the average plutonium concentration in the ducts. Uncertainties in those relationships were propagated through the release estimate calculation along with the estimates of bias reported in Phase I. The median bias factor was taken to be a constant (1.3) over time, but the GSD of the bias factor was somewhat greater (1.6) for the period 1953–1973 from that for later years (1.4).

Effluent was passed through high-efficiency particulate (HEPA) filtration before discharge to the atmosphere. The median particle size for HEPA filtered effluent was reported to be 0.3 μm [Voillequé (1999)]. However, when filter leakage occurred, larger particles (more typical of the workplace aerosols) would have been released. For this reason routine operational releases were assumed to be characterized by a plutonium aerosol with an AMAD of ~1 μm and a GSD of 2.5 (Voillequé 1999).

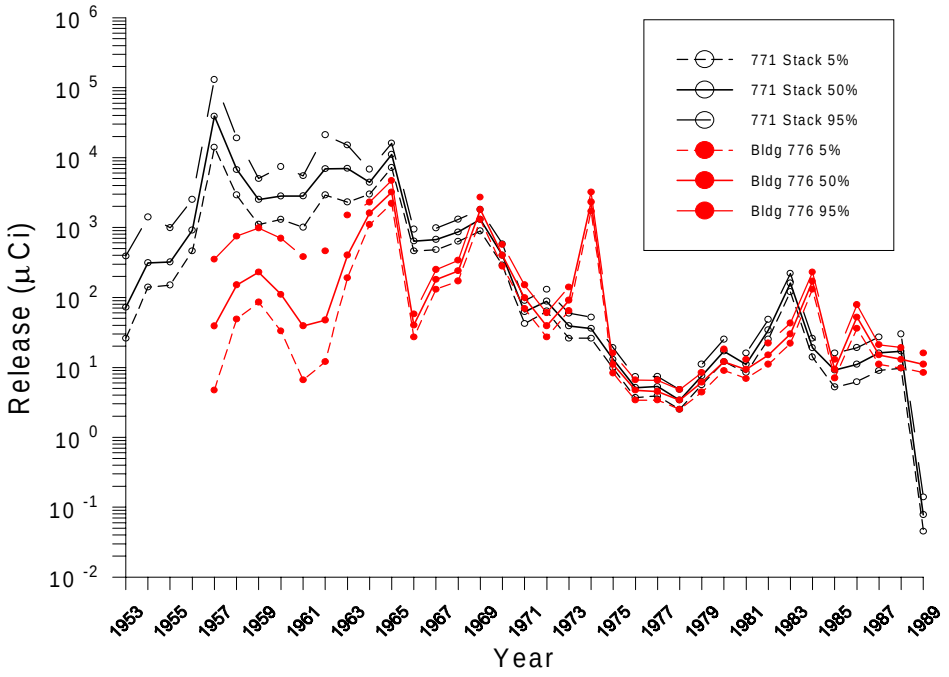

Figure 2. Estimates of routine plutonium releases from Building 771 stack and Building 776/777 roof vents. Releases from the major fires in 1957 and 1969 are not included. Taken from Voillequé (1999).

Median release estimates and the 5th and 95th percentile values for Building 771 stack and Building 776/777 roof vents are illustrated in Figure 2. Prior to 1963, releases were dominated by the Building 771 stack. Highest releases were estimated to be in 1957, the year of the fire in Building 771. Release estimates for that year ranged from 14,000 μCi (5th percentile) to 130,000 μCi (95th percentile) and were due primarily to the extended clean-up work that followed the

accident. Releases as a direct result of the two major fires in 1957 and 1969 are not included in these estimates. Uncertainty in release estimates varies from year to year and is greatest for the early years of plant operation.

ENVIRONMENTAL MONITORING OF PLUTONIUM

Historical environmental monitoring data are evaluated in Rope et al. (1999). In this section we briefly review the data that are pertinent to routine releases of plutonium, emphasizing data that may potentially be used for model validation. This limits our discussion to measurements of ambient air and ground deposition. In general, we found air monitoring data to be of little use for validating model predictions because;

- Air monitoring prior to 1970 only measured total alpha or total long-lived alpha activity. Natural background, weapons fallout, poor detection limits, and other more significant sources such as the 903 Area in the mid to late 1960s obscured the impact of routine releases at the samplers.
- After 1970, plutonium specific analyses were made but these measurements were again obscured by releases from contaminated areas east of the 903 Area.

Ambient Air Monitoring

A detailed review and analysis of plutonium monitoring in air around Rocky Flats is documented in Rope et al. (1999). Air monitoring was performed by the site contractor and several independent agencies. Before 1970, samplers were only analyzed for total long-lived alpha activity (TLLa). The RFP contractor began onsite ambient air monitoring at a single station in 1952. By early 1953, 10 onsite stations had been established and in 1969, two additional stations were added. In the 1950s (particularly 1955–1960), 4-hour gross alpha counts were made. The count was made 4 hours after collection and included large contributions from natural alpha emitting radionuclides like radon decay products. Rope et al. (1999) concludes that the 4-hour count results are of no value in assessing the concentrations of long-lived alpha emitters released from Rocky Flats.

Beginning in January 1960, 1-week counts and 4-hour counts of alpha and beta activity were performed. The 1-week count was performed 1-week after sample collection resulting in decay of most of the short-lived radon progeny and thereby providing a measure of the long-lived alpha activity collected on the filter. Results were summarized in monthly sampling reports that reported the maximum and minimum average activity levels at all samples for that month. Daily sampling sheets were obtained from 10 October, 1964 to 29 December, 1971 for samplers S-1 through S-10 (with the exception of S-9). The minimum detectable concentration quoted by the site contractor was 0.21 counts per minute (cpm) which equates to an activity concentration of 5.5 fCi m^{-3} TLLa (Rope et al. 1999). A conversion factor of 0.038 cpm fCi^{-1} m^3 was used in the calculation. The plutonium activity concentration in ambient air resulting from weapons fallout for the 1960–1970 time frame is around 0.1 fCi m^{-3} and the long-term average background from natural sources of long-lived alpha activity is 1.4 fCi/m^{-3} (Rope et al. 1999) but can be as high as 7–10 fCi/m^{-3} (Rope et al. 1999) on any given day.

In 1964, the first indication that drums containing plutonium contaminated cutting oil and stored on what is now known as the 903 Area (Meyer et al. 1996) were leaking and

contaminating the underlying soil. Suspension of this soil by wind and man-made disturbances was detected in 12 onsite samplers, particularly the S-8 sampler located east of the 903 Area. This airborne source is believed to have dominated the activity measured at onsite and offsite sampling locations from 1964 to the present. Annual average concentrations of TLLa in samplers S-1 – S-51 in 1969 (the year of highest measured concentrations) ranged from 4–185 fCi m^{-3}. With the exception of sampler S-7 and S-8, most samplers had annual average concentrations at or slightly above the minimum detectable concentration of 5.5 fCi m^{-3}.

In 1970, several independent agencies began air monitoring in the vicinity of the RFP. These agencies included the Health and Safety Laboratory of the Atomic Energy Commission (HASL), Colorado Department of Health, and U.S. Environmental Protection Agency (EPA). Analytical methods included plutonium specific analysis for air filters. Annual average concentrations for 1970–1981 above expected fallout concentrations were observed at 4 monitoring stations located on the eastern security fence, the old RFP boundary, Indiana Street, and 6.6 km (4 miles) west in Coal Creek Canyon. Hardy (1972) concluded that the only significant source of plutonium contamination around Rocky Flats originated from the leaking drums on the 903 Pad based on studies of plutonium isotopic ratios. They argued if routine stack emissions were a significant source, then the content of the short-lived ^{241}Pu would be much greater. Upwind-downwind sampler studies by Hodgin (1984) and Hammer (1984) also indicated the primary source of plutonium in ambient air after 1970 was from resuspension from the field east of the 903 Area. Based on these observations, it is unlikely plutonium originating from routine operations was an appreciable component of plutonium concentrations measured in samplers after 1970. For these reasons, model validation of routine releases after 1970 is not possible without knowing the contributions from other sources including resuspension of plutonium contaminated soil from the field east of the 903 Pad. In addition, other sources of plutonium such as the solar evaporation ponds may have contributed plutonium in ambient air measured during the 1960s. Release estimates for these sources were not developed. For these reasons, comparisons of model predictions with measurements are not discussed in this report. A comprehensive model validation that includes all potential plutonium sources is reported in Rood and Grogan (1999).

Deposition Measurements Using Gummed-Paper Collectors

Examination of gummed-paper collectors that were used to measure fallout radioactivity at and around the RFP is described in Rope et al. (1999). Gummed-paper collectors were used periodically during the years 1954–1972. Measurements were specifically made for plutonium. The earliest references to fallout monitoring were found in the 1954 site survey reports, although no data were reported. Fallout monitoring is not mentioned again in the site survey reports until May 1963. Data were found for the following periods: (1) May 1963 through June 1964, (2) May 1965 through December 1965, and (3) January 1970 through June 1972. Deposition measurements made from 1965 to the mid 1970s were probably strongly influenced by releases from the 903 Area, therefore, it is unlikely fallout from routine releases would be detected during these years. In addition, plutonium from weapons fallout often was a significant contribution to the total activity collected. As mentioned in the previous section, other sources of plutonium such as resuspension of plutonium from 903 Area, and solar evaporation pond sediments may have impacted sampling results in previous years. For these reasons, comparison of gum-paper

collector results was dismissed in a separate report (Rood and Grogan 1999) that integrates all the major atmospheric releases of plutonium from RFP.

ENVIRONMENTAL TRANSPORT MODELING

Offsite exposure to plutonium from routine releases at RFP was investigated in Phase 1 and summarized in a previous section. Airborne releases were considered to be the dominant transport pathway and inhalation the major pathway of exposure.

Atmospheric releases of plutonium during routine operations at the RFP primarily occurred from two release points; roof vents on Buildings 776 and the 44 m stack from Building 771. Other minor release points were also identified in Phase I reports (ChemRisk 1994a). In this section, we describe our approach to estimating atmospheric dispersion of plutonium for the years 1953–1989 and the uncertainty associated with concentration estimates in the model domain. Our approach to this calculation involves first estimating an annual average X/Q (concentration divided by source term [s m^{-3}]) for each receptor in the model domain. Concentrations for specific years of the assessment period are calculated by multiplying the annual quantity of plutonium released to the atmosphere by the X/Q value for a given receptor located in the model domain. Uncertainties in dispersion estimates are accounted for through multiplicative correction factors. Airborne concentrations are then used with exposure scenarios and the risk coefficients to calculate lifetime cancer incidence risk for selected receptors in the model domain.

Atmospheric Model Selection

Five atmospheric transport models were considered for use in this study, and were evaluated in Rood (1999):

1. Terrain-Responsive Atmospheric Code (TRAC) (Hodgin 1991)
2. Industrial Source Complex Short Term Version 2 (ISC) (EPA 1992)
3. Regional Atmospheric Transport Code for Hanford Emission Tracking (RATCHET) (Ramsdell et al. 1994),
4. TRIAD (Hicks et al. 1989)
5. INPUFF2 (Petersen and Lavdas 1986).

The purpose of the model comparison study was to determine what models, if any, performed best in the Rocky Flats environs for a given set of modeling objectives. These data along with other studies were used to establish the uncertainty one might expect from a model prediction.

Model evaluations were based on how well predictions compared with measured tracer concentrations taken during the Winter Validation Tracer Study (Brown 1991) conducted in February 1991 at the RFP. The study consisted of 12 separate tests; 6 tests were conducted during nighttime hours, 4 during daytime hours, and 2 during day-night transition hours. For each test, an inert tracer (sulfur hexafluoride) was released in an open area near the southern RFP boundary. The tracer was released at a constant rate for 11 hours from a 10 m high stack. Two sampling arcs, 8 and 16 km from the release point, measured tracer concentrations every hour for the last 9 hours of each test period. Seventy-two samplers were located on the 8-km arc, and 68 samplers were located on the 16-km arc. Predicted concentrations were then compared to the observed tracer concentrations at each of the samplers.

Modeling objectives for the comparison study were based on the premise that identifying locations of individual receptors on an hour-by-hour basis was unlikely. Instead, it was more likely to identify receptors (hypothetical or real) who were present at a fixed location for the duration of a release event. The minimum time scale of historical release events at RFP ranged from one to several days. Release events modeled for the Winter Validation Tracer Study were 9 hours in duration. If we assume the receptor is fixed for a time period of at least 9-hours, then the time-averaged concentration (9-hour average) rather than the hourly average concentration is the appropriate modeling objective. Therefore, models were evaluated based on their performance in predicting time-averaged concentrations at fixed sampler locations in the model domain (9-hour average concentration at each sampler paired with the corresponding predicted value). Data sets for the time-averaged concentration were limited to only those points where the predicted (C_p) and observed (C_o) concentration pair were greater than the time-averaged minimum detectable concentration.

Fifty percent of the time-averaged model predictions were within a factor of 4 of the observations. Predicted-to-observed ratios (C_p/C_o) ranged from 0.001 to 100 and tended to be higher at the 16-km arc than the 8-km arc. Geometric mean C_p/C_o ratios ranged from 0.64 (TRAC) to 1.5 (ISC), and GSDs ranged 4.4 (RATCHET) to 6.5 (ISC). The RATCHET model had the highest correlation coefficient for the 8-km (0.67) and 16-km (0.58) sampling arc followed by TRIAD and INPUFF2 (Figure 3). Qualitatively, the predictions made by the RATCHET model appear to match the observations best. The slope of the regression line was closest to that of the perfect correlation line (solid line in Figure 3).

The results reported in Rood (1999) indicated that no one model clearly outperformed the others. However, the RATCHET, TRIAD, and INPUFF2 models generally had lower variability (indicated by lower GSDs of C_p/C_o ratios) and higher correlation coefficients compared to those of ISC and TRAC models. It is desirable in a study such as this to choose a model that has the least amount of variability when comparing model predictions to observations. In addition, the model selected should have a level of complexity that is consistent with available data. The TRAC model is the most complex in terms of its treatment of the atmospheric dispersion process in complex terrain, but the study showed model performance was no better than the other models. In addition, the availability of meteorological data needed to fully use the capabilities of the TRAC model are lacking. The straight-line Gaussian plume model, ISC tended to overpredict concentrations and was also limited to only one meteorological recording station in the model domain. Available meteorological data for this study period included two meteorological recording stations; one at the RFP and the other at Denver Stapleton International Airport. Therefore, a model that may include multiple meteorological recording stations in the model domain is desirable. The use of multiple meteorological recording stations allows a spatially varying wind field in the model domain.

The three models RATCHET, INPUFF2, and TRIAD performed comparably and were considered viable candidates for atmospheric dispersion estimates. We chose the RATCHET model for modeling routine releases of plutonium for the following reasons:

- The model was easily configured for long-term (annual average) dispersion estimates
- Spatial differences within the model domain are accounted for (i.e., surface roughness meteorology)
- Algorithms to compute plume depletion and deposition for fine particles are included (deposition must be computed outside the TRIAD and INPUFF2 codes)

- The model requires meteorological data in 1-hour increments, which are the same as those given for typical airport observations.

Corrections for model bias were made in the uncertainty analysis. Features of the RATCHET model are summarized in Table 1.

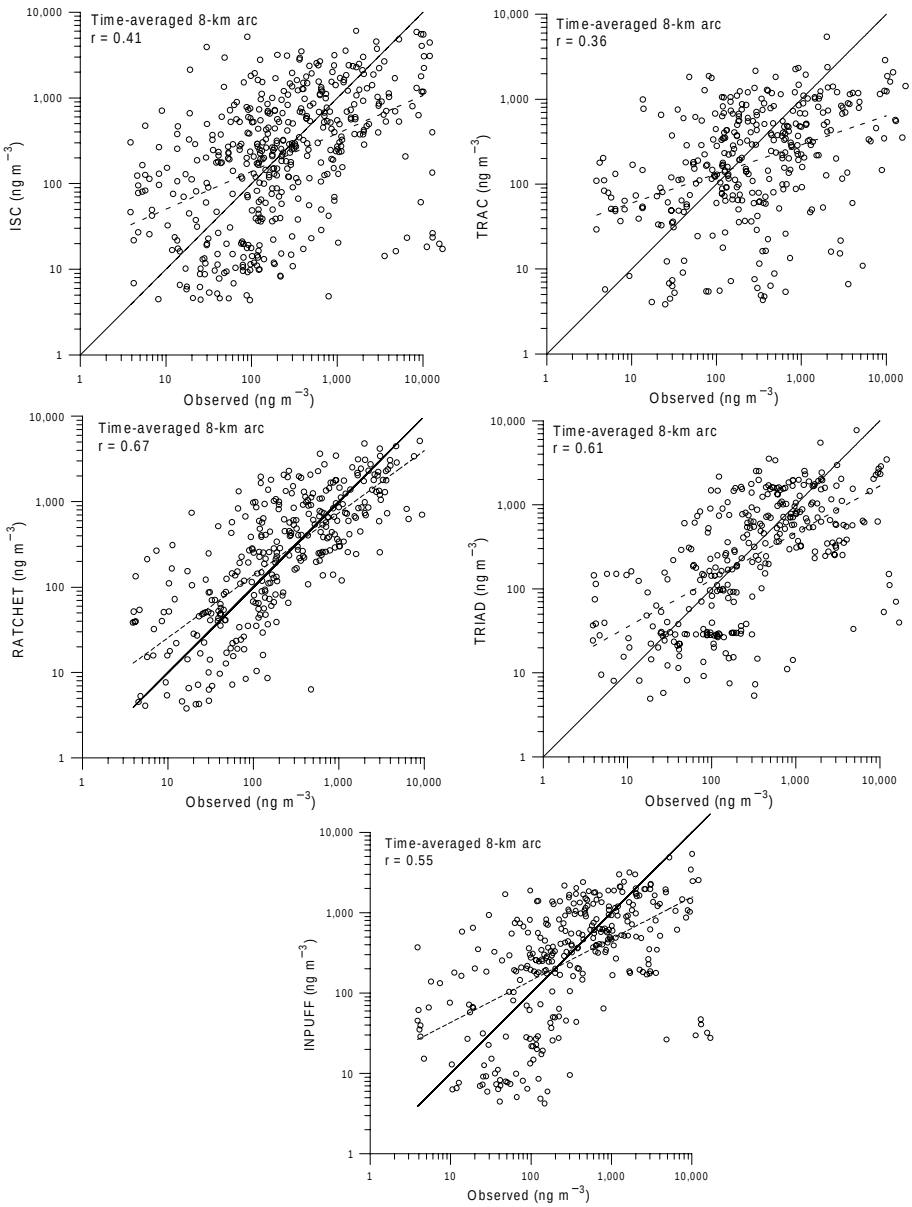

Figure 3. Nine-hour average observed concentrations as a function of predicted values for the five models compared using the Winter Validation Tracer Study data set. Correlation coefficients were for the log-transformed data. The solid line represents perfect correlation between predicted and observed values. The dashed line represents the log-transformed regression fit.

Table 1. Features of the RATCHET Model

Feature	Representation in RATCHET
Domain area[a]	2,100 km^2
Node spacing[a]	2,000 m
Source term	Hourly release rates
Meteorological data	Hourly
Surface roughness	Spatially varying
Wind fields	1/r^2 interpolation
Topographical effects	None explicit[b]
Wind profile	Diabatic
Stability	Spatially varying based on wind, cloud cover, and time of day
Precipitation	Spatially varying, three precipitation regimes with different precipitation rate distributions
Mixing layer	Spatially varying, based on calculated values for each meteorological station
Plume rise	Briggs' equations (Briggs 1969, 1975, 1984)
Diffusion coefficients	Based on travel time and turbulence levels
Dry deposition	Calculated using resistance model
Wet deposition	Reversible scavenging of gases, irreversible washout of particles
Model time step	15 minute maximum, 15 second minimum
Output frequency[c]	Daily
Uncertainty	Options available for Monte Carlo simulation within the code

[a] Modified from the original RATCHET specification for use at Rocky Flats.

[b] The model does not account for terrain elevation changes relative to the plume height explicitly. However, topographical influence on the wind field may be accounted for by incorporating multiple meteorological stations in the model domain.

[c] Modified to output annual average concentrations at user specified grid nodes.

Model Domain and Receptor Grid

The model domain (Figure 4) encompasses a 2,200 km^2 area (50 km north-south by 44 km east-west). The domain extends 28 km south, 12 km west, 22 km north, and 32 km east from the RFP. Most of the Denver metropolitan area and the city of Boulder are included in the domain. The domain was limited in its western extent because few receptors are present there and most of the contaminant plumes traveled east and southeast of the plant.

RATCHET uses two modeling grids, an environmental grid and a concentration grid. The wind speed and direction, stability, precipitation and surface roughness features are estimated on the environmental grid using the hourly meteorological records. The concentration grid has spacing one-half that of the environmental grid. Ground-level plutonium concentrations in air and plutonium deposition are output at each of these grid nodes. The environmental grid has a grid spacing of 2,000 m with 23 nodes east-west and 26 nodes north south. The concentration grid has a grid spacing of 1,000 m with 45 nodes east-west and 51 nodes north-south. The southwest corner of the model domain has the universal transverse mercator (UTM) coordinates 470850 E and 4387050 N. Plutonium release points are defined by distances (in kilometers) from

a reference node. The reference node for the environmental grid was (7,15) and (13,29) for the concentration grid and both have the UTM coordinates of 482850 E and 4415050 N.

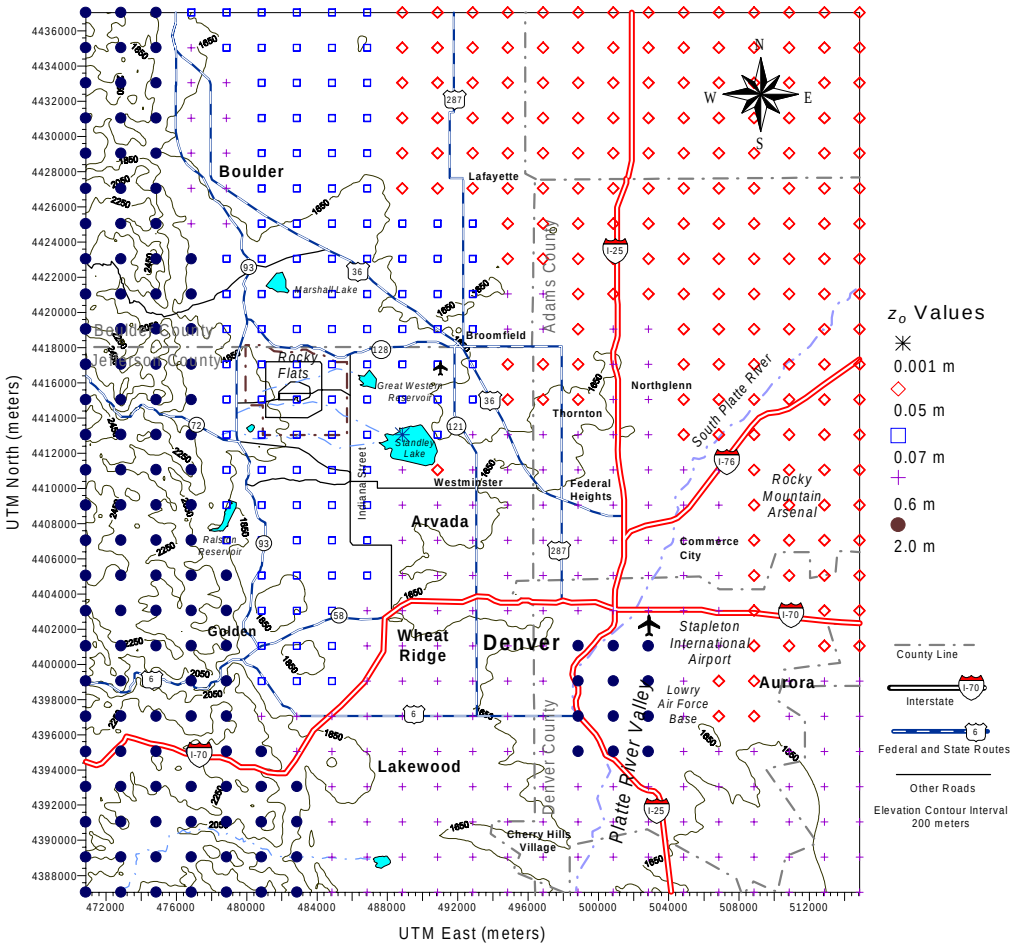

Figure 4. RATCHET environmental modeling grid and roughness length values (z_o). Symbols represent grid nodes and the z_o value assigned to the node.

Figure 4 was generated using United States Geological Survey (USGS) 7.5-minute digital elevation models. Topographic contours were based on an elevation grid spacing of 100 m. Major roadways were digitized from United States Geological Survey (USGS) 1:100,000 digital line graphs.

Meteorology

Meteorological data for the operational period of Rocky Flats (1953–1989) are sporadic, incomplete, and of questionable integrity. Requests for meteorological data from the RFP were initially made by ChemRisk during Phase I of the project. ChemRisk was able to locate two letters from Dow Chemical to Dr. Roy Cleare, Executive Director of the Colorado Department of Health, dated March 20, 1970, that contained wind speed and direction for varying time

increments during the 1957 and 1969 fire incidents. Computer diskettes containing wind speed, wind direction, and precipitation measurements from October 1968 to May 1969 were also obtained. These data were hourly observations taken approximately 15 minutes before the top of the hour and do not represent hourly average readings. Although these data appeared to be climatologically reasonable, no records of instrument calibration or audits of the information were found. Parameter resolution was very coarse (for example, wind direction resolution was 45 degrees). Five years (1987–1991) of high quality meteorological data taken at the 61-m tower at RFP were obtained and used by ChemRisk in Phase I of this project for predicting annual average concentrations from routine releases.

An extensive data search was initiated in 1994 by *Radiological Assessments Corporation (RAC)* researchers to locate missing data and interview personnel who were involved with measurements at the site. No new data were recovered, but several personnel reported problems with the recording instrumentation at the RFP, such as the measured wind direction being off by 180 degrees. Other data recorded from nearby Jefferson County Airport (about 8 km east of the plant) were obtained for the years 1968–1971. These data were only reported for the hours while the airport was open (06:00–23:00 local standard time) and were instantaneous measurements and not hourly averages as was typical of all airport data before the Automatic Surface Observation Site system was installed at most major airports. In 1994, the RFP hired a subcontractor to compile, screen, validate, and analyze historical climatological data (DOE 1995). A draft report was issued in February 1995; the report contained monthly and annual summaries of wind speeds, wind directions, precipitation, temperature, and other parameters for the years 1953–1993. While these data are of interest and may be important for some aspects of modeling, they lacked the resolution required for detailed atmospheric transport modeling.

We concluded that meteorological data taken during the time the RFP was operating were incomplete, unreliable, and unsuitable for atmospheric transport modeling during the period 1953–1989. However, surrogate data spanning a different time period can be used to make annual average dispersion estimates for past releases. We used this approach in our modeling effort.

For our modeling effort, we used meteorological data spanning a 5-year period (1989–1993) taken at two recording stations located at the RFP and Denver Stapleton International Airport. Federal regulations have stated a 5-year database is adequate for predicting annual-average air quality impacts at a site (CFR 1996). How representative this 5-year data set is for earlier time periods is discussed in the uncertainty section. Meteorological data from RFP were taken at the 10-m level from the 61-m tower located on the south side of the plant complex at UTM coordinates 482064 E 4414963 N. Data recorded at this station included wind speed, wind direction, temperature, and other parameters (heat flux and standard deviation of wind direction) that were not used in these simulations. The Denver Stapleton International Airport meteorological station was located 24 km east and 14 km south from the center of the model domain (RFP). These data included hourly measurements of wind speed, wind direction, cloud cover, and precipitation. It is known that meteorological conditions in the Denver metropolitan area can differ significantly from those at Rocky Flats (DOE 1980). Therefore, it is unreasonable to use meteorological data from Denver alone for simulations involving releases from Rocky Flats. In these simulations, initial plume trajectories are primarily influenced by the wind direction at Rocky Flats. Only after plume elements are transported to the Denver metropolitan area are trajectories and dispersion influenced by meteorological conditions present there.

Data Processing

Meteorological data from 1989–1993 were obtained in electronic format from the Rocky Flats meteorologist. These data were measured at a height of 10 and 61-m from a 61-m tower located at RFP. Only data from the 10-m level were used in the simulations. Each record represented the average over a 15-minute recording period and included wind speed and direction, temperature, heat flux, and standard deviations of these parameters. Processed data suitable for use in EPA's ISC code were also obtained for the same time frame. These data included stability class estimated by the lateral turbulence and wind speed method (standard deviation of the horizontal wind direction fluctuations) as described in EPA (1987) and mixing height estimates. The mixing heights were derived from linear interpolation for each 15-minute period from the rawinsonde data furnished routinely every 12 hours by the National Weather Service for Denver Stapleton International Airport. These data were used as default mixing-layer depths in RATCHET. Mixing-layer depths are calculated hourly within RATCHET at each active meteorological recording station using a methodology described by Zilitinkevich (1972). The calculated or default value is selected on the basis of the relative magnitude of the calculated and default values, the stability, season, and time of day. The larger of the two is selected for the meteorological recording station for the given hour. A multiple linear regression technique is then used to provide a smooth spatial variation in mixing-layer depth across the model domain.

Stability classes were calculated separately for the RFP and Denver Stapleton International Airport meteorological recording stations using the general classification scheme discussed in Pasquill (1961), Gifford (1961), and Turner (1964). This typing scheme employs seven stability categories ranging from A (extremely unstable) to G (extremely stable) and requires estimates of sky cover and ceiling height. Cloud cover and ceiling height data for both stations were assumed to be the same and were obtained from the Denver Stapleton International Airport data.

Hourly average wind speed and direction also were calculated from the raw RFP meteorological data using the protocol described in EPA (1987). An arithmetic average of the wind direction was computed first, and it was then segregated into 1 of 36, 10-degree increments as required by RATCHET. The average wind speed for the hour was computed by taking the average of the four, 15-minute data segments. Hourly precipitation records from Denver Stapleton International Airport were assumed to be consistent over the entire model domain and were segregated into integer values as required by RATCHET (see Table 3).

Atmospheric Transport Model Parameters

This section describes the input parameters that were selected for the RATCHET model for simulations involving normal operational releases. These parameters include surface roughness length, topography, dry and wet deposition, diffusion coefficients, release parameters (location and height of release), and model control parameters (number of puffs per hour and computational options).

Surface Roughness Length

Roughness elements (such as trees and buildings) and small-scale topographic features (such as rolling hills) have a frictional effect on the wind speed nearest the surface. The height and spacing of these elements determine the frictional effects on the wind. These effects are directly related to transport and diffusion, and affect atmospheric stability, wind profiles, diffusion coefficients, and the mixing-layer depth. The surface roughness length parameter is used to describe these roughness elements and is a characteristic length associated with surface roughness elements (Table 2). In RATCHET, estimates of the surface roughness length are defined for each node on the environmental grid (Figure 4). In our simulations, we selected a value of 0.6 m to represent residential and urban environs. Farmland, which is predominant in the northeast part of the model domain, was assigned a value of 0.05 m. Range and open land consisting of rolling grass hills were assigned a value of 0.07 m. Nodes that encompass the range and farmland designation were selected based on the topographic contours and land use maps. The foothills and downtown Denver were assigned a value of 2.0 m and open water (Standley Lake) was assigned a value of 0.001 m.

Table 2. Typical Surface Roughness Lengths for Different Land Use, Vegetation, and Topographic Characteristics[a]

Land use, vegetation, and topographic characteristics	Surface roughness length, z_o (m)
Level grass plain	0.007–0.02
Farmland	0.02–0.1
Uncut grass, airport runways	0.02
Many trees/hedges, a few buildings	0.1–0.5
Average, North America	0.15
Average, U. S. Plains	0.5
Dense forest	0.3–0.6
Small towns/cities	0.6–2.5
Very hilly/mountainous regions	1.5+

[a] Source: Stull (1988), Figure 9.6

Topography

The RATCHET model does not explicitly address terrain differences within the model domain. Instead, topography and topographic effects on transport and diffusion are reflected in the surface roughness lengths and observed wind velocity data that are affected by topographical features. Topography in the model domain (Figure 4) can be characterized by three major features: the north-south trending Colorado front range foothills in the western part of the model domain, the southwest to northeast trending Platte River Valley located in the southeast part of the model domain, and rolling hills and flat farmland that is predominant in the central and northeastern part of the model domain. The topography generally slopes east from Rocky Flats dropping 200 m in elevation to the Platte River Valley. The surface roughness lengths reflect these features as stated in the previous section. Observed meteorological data are lacking in most

of the model domain and are woefully inadequate to characterize wind fields in the foothills region. However, meteorological observations at Denver Stapleton International Airport do capture the air movement within the Platte River Valley, which is noticeably different than that at the RFP (DOE 1980). Therefore, to a limited extent, topography is accounted for the model simulation. The use of a complex terrain model would also suffer from the lack of meteorological data, especially in the foothills region. This region is of lesser importance because few receptors were present in the foothills when the plant was operating.

Dry and Wet Deposition

Dry and wet deposition processes are used to deplete contaminant mass from the plume as it traverses the model domain and estimate surface concentrations of deposited material. Surface concentrations were calculated for each concentration node in the model domain. However, these values were not used the exposure assessment but were stored and may be used in a later assessment. The rate of deposition of small particles on surfaces in the absence of precipitation is proportional to the concentration of material near the surface. The proportionality constant between the concentration in air and the flux to the ground surface is the dry deposition velocity. The current generation of applied models estimates deposition using an analogy with electrical systems as described by Seinfeld (1986). The deposition is assumed to be controlled by a network of resistances, and the deposition velocity is the inverse of the total resistance. Resistances are associated with atmospheric conditions; physical characteristics of the material; and the physical, chemical, and biological properties of the surface. The total resistance in RATCHET is made up of three components: aerodynamic resistance, surface-layer resistance, and transfer resistance. Thus, the dry deposition velocity (v_d, m s^{-1}) is calculated using

$$v_d = (r_s + r_a + r_t)^{-1} \quad (1)$$

where
r_s = surface layer resistance (s m^{-1}),
r_a = aerodynamic resistance (s m^{-1}),
r_t = transfer resistance (s m^{-1}).

Surface layer resistance and aerodynamic resistance are given by

$$r_a = U(z)/u_*^2 \quad (2)$$

$$r_s = 2.6/(0.4\, u_*) \quad (3)$$

where u_* = frictional velocity (m s^{-1}), and $U(z)$ = wind speed (m s^{-1}) measured at height z (m) above the ground.

The frictional velocity is given by

$$u_* = \frac{U(z)\, k}{\ln(z / z_o) - \psi(z / L)} \quad (4)$$

where

k = the von Karman constant (0.4),
z_o = surface roughness length,
ψ = stability correction factor, and
L = the Monin-Obukhov length (m).

The transfer resistance is associated with the characteristics of the depositing material and surface type. In RATCHET, the transfer resistance is used as a mathematical means to place a lower limit on the total resistance. As the wind speed increases, r_s and r_a become small resulting in unreasonably high deposition velocities. For small particles (<1.0 μm), a transfer resistance of 100 s m^{-1} is suggested in RATCHET, and it results in calculated deposition velocities that are consistent with measured data. Harper et al. (1995) estimates deposition velocities for 1-μm particles and 5 m s^{-1} wind speed to range from 1.0×10^{-2} (5^{th} percentile) to 4.1 cm s^{-1} (95^{th} percentile). The RATCHET calculated values assuming a roughness length of 0.05 m and a transfer resistance of 100 s m^{-1} ranged from 0.66 to 0.75 cm s^{-1}, which is in the range of measured values.

Gravitational settling (v_t) is not included in Equation (1) but may be added. However, for small particles (~1.0 μm), gravitational settling is negligible compared to r_s and r_a. Stokes law gives the gravitational settling velocity for particles less than 20 μm as

$$v_t = \frac{C_c d^2 g \rho}{18 \mu_{air}} \quad (5)$$

where
C_c = the Cunningham slip correction factor (dimensionless),
d = particle diameter (cm),
g = gravitational acceleration constant (980 cm s^{-2}),
μ_{air} = dynamic viscosity of air (1.78×10^{-4} g s^{-1} cm^{-2}),
ρ = particle density (11.46 g cm^{-3} for plutonium).

For particle sizes less than several microns, the Cunningham Slip correction factor is approximately 1.0. Figure 5 presents gravitational settling velocity as a function of particle size. Effluent containing plutonium was reported to pass through HEPA filtration resulting in release of particle less than 1 μm in diameter. Median particle size has been estimated to be 0.3 μm (Voillequé 1999). Whicker and Schultz (1982) report that gravitational settling velocities for particles less than 1 μm are insignificant compared to the other components of deposition. Deposition velocities calculated using Equation (1) ranged from 0.3 to 1.0 cm s^{-1}, for wind speeds ranging from 2.5 to 20 m s^{-1}, roughness lengths from 0.001 to 2 m, and a transfer resistance of 100 s m^{-1}. Note that the gravitational settling velocity for 0.3 μm particles (≈0.006 cm s^{-1}) is insignificant compared to the deposition velocity calculated with Equation (1). For our simulations, gravitational settling was ignored and a transfer resistance of 100 s^{-1} m was used.

Wet deposition of small particles in RATCHET is modeled using a washout coefficient and assuming irreversible collection of particles as the precipitation falls through the puffs. The following expression discussed in Slinn (1984) is used to compute the washout coefficient in RATCHET:

$$\Lambda = \frac{C\,E\,P_r}{0.35\;P_n^{1/4}} \tag{6}$$

where

Λ = washout coefficient (hr^{-1}),
C = empirical constant assumed to have a value of 0.5,
E = average collision efficiency assumed to be 1.0,
P_r = precipitation rate (mm hr^{-1}),
P_n = normalized precipitation rate (P_r)/ [1 mm hr^{-1}]).

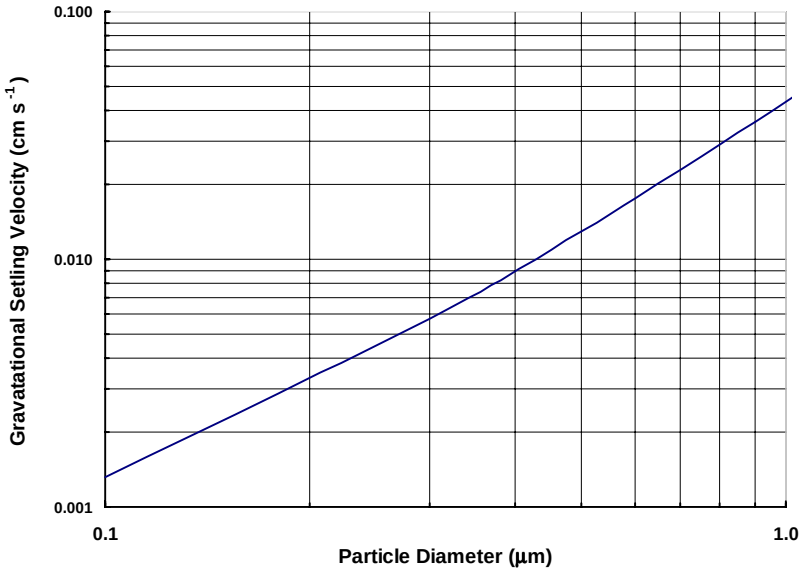

Figure 5. Gravitational settling velocity as a function of particle diameter for plutonium (ρ = 11.46 g cm^{-3}).

The normalized precipitation rate is a dimensionless quantity that represents the precipitation rate normalized to 1 mm h^{-1}. During periods of snow, the washout coefficient for particles is computed by

$$\Lambda = 0.2\,P_r. \tag{7}$$

Precipitation rates in RATCHET are separated into six classes: three for liquid and three for frozen precipitation (Table 3). These classes are the similar to those reported by most airport meteorological recording stations.

Table 3. Precipitation Rates and Washout Coefficients Used in RATCHET

Precipitation type	Precipitation rate (mm hr^{-1})	RATCHET precipitation code	Washout coefficient (hr^{-1})
No precipitation	0.0	0	0.00
Light rain	0.1	1	0.254
Moderate rain	3.0	2	3.26
Heavy rain	5.0	3	4.78
Light snow	0.03	4	0.006
Moderate snow	1.5	5	0.3
Heavy snow	3.3	6	0.66

Diffusion Coefficients

The RATCHET model estimates the diffusion coefficients directly from statistics for atmospheric turbulence. In most cases, the statistics describing atmospheric turbulence (i.e., standard deviation of the horizontal and vertical wind direction fluctuations) are not routinely measured at most meteorological recording stations. However, RATCHET makes use of atmospheric conditions that are either measured or calculated from routine meteorological data to estimate the turbulence statistics. The parameters wind speed, atmospheric stability, and surface roughness are used to estimate the turbulence statistics. The general form of the equation used in RATCHET for estimating the horizontal diffusion coefficient (σ_r) for the first hour following release is

$$\sigma_r = 0.5\sigma_v\, t \tag{8}$$

where

σ_v = crosswind component of turbulence (m s^{-1}) and

t = travel time.

After the first hour, the horizontal diffusion coefficient is given by $\sigma_r = c_{sy}\, t$ where c_{sy} is a proportionality constant with dimensions of meters per second. Gifford (1983) has shown the value of c_{sy} distributed between 0.14 to 1.4 with a median value of 0.5. For our simulations, we used the median value of 0.5.

The general form of the equation for estimating the vertical diffusion coefficient (σ_z), near the source is

$$\sigma_z = \sigma_w\, t\, f_z(t) \tag{9}$$

where

σ_w = standard deviation of the vertical component of the wind (m s^{-1}),

$f_z(t)$ = nondimensional function related to the travel time and turbulence time scale.

As a practical matter, diffusion coefficients in RATCHET are calculated in increments to avoid problems associated with spatial and temporal changes in conditions.

Source Characterization

Estimated releases of plutonium to the atmosphere were provided by Voillequé (1999) and are summarized in a previous section. Release estimates were tabulated separately for Buildings 776 and the 771 stack. Model release parameters are described in Table 4. Releases from Building 776 originated from nine roof vents. ChemRisk (1992) reports the flow rates, velocities, and geometry of these vents in their Task 3 and 4 reports. Two of the vents were inverted "J" type. One vented to a conical hat about 15 feet above the roof and the remainder were a louvered rectangle penthouse type, 3.3 ft high above the roof, and vented on all 4 sides. Because the effluent was diverted vertically, no momentum driven plume rise was modeled for releases from Building 776.

The building height was 11.6 m and the horizontal dimensions were 61 × 104 m. The vents were assumed to be distributed across the roof resulting in an area source geometry. The area source was simulated by modifying the initial diffusion coefficients using a procedure described by Petersen and Lavdas (1986). The initial horizontal diffusion coefficient (σ_r) is the horizontal dimension of the source divided by 4.3, and the initial vertical diffusion coefficient (σ_v) is the height of the source divided by 2.15. For these simulations, we used the 61-m length as the horizontal source dimension. No momentum or buoyant driven plume rise was assumed.

Atmospheric releases of plutonium from the Building 771 assumed the effluent passed through HEPA filtration as described previously and exited out the top of the 44-m stack with an exit velocity of 11.7 m s^{-1}. An average release temperature of 20° C was assumed.

Table 4. Release Parameters for Building 771 Stack and Building 444

Release Point	Parameter	Value
Building 771 Stack	Stack height	44 m
	Stack diameter	3.05 m
	Flow rate[a]	87 m^3 s^{-1}
	Effluent Temperature	20° C
	UTM east	482870 m
	UTM north	4415870 m
Building 776 roof vents	Release height	11.6 m
	Initial σ_r	14.1 m
	Initial σ_v	5.4 m
	UTM East	482825 m
	UTM North	4415740 m

a. Flow rate was based on 184,000 actual cubic feet per minute as reported in the Phase 1 reports (ChemRisk 1994b)

Stack tip downwash is also modeled in RATCHET; however, building wake is ignored. Building wake is important for buildings within 2.5L of the stack where L = the lesser of the building height or width (EPA 1985). The closest building to the 771 stack is Building776 (≈50 m) which has a height of about 12 meters and beyond the 2.5L distance from the stack. Moreover, building wake affects only those receptors relatively close to the source. At distances of about 2 km, building wake has been shown to have little affect on measured atmospheric concentrations (Start et al. 1980). Ramsdell (1990) showed that for ground-level releases,

modeled air concentrations greater than 1 km from the source are relatively unaffected by building wakes. Note the nearest receptor is >3 km from the 771 stack.

Uncertainty associated with the source term was incorporated on a year-by-year basis in the source term estimates. Uncertainty was represented by separate distributions for each year reported (1953–1989). Details of each distribution are found in Voillequé (1999).

Other Parameters

Several other parameters in RATCHET influence the accuracy of output and computer runtime. These parameters include the number of puffs per hour, minimum time step, puff consolidation, maximum puff radius, and minimum puff concentration at center. We chose the suggested RATCHET default values for all these parameters except minimum time step and minimum concentration at puff centers (Table 5). Accuracy of the simulation can be improved by using a smaller time step. The RATCHET default was 20 minutes, which we reduced to 10 minutes. The minimum concentration at puff centers was reduced from 1×10^{-13} to 1×10^{-15} to allow for plume tracking throughout the model domain. The puff consolidation parameter value combines puffs from the same source when ratio of the puff centers to the average σ_r is less than the user-input value. The puff consolidation ratio and maximum puff radius (in units of σ_r) were set at RATCHET default values of 1.5 and 3.72, respectively.

Table 5. RATCHET Model Control Parameters

Model parameter	Value
Number of puffs per hour	4
Minimum time step	10 minutes
Puff consolidation	1.5
Maximum puff radius (in units of σ_r)	3.72
Minimum concentration at puff centers	1×10^{-15}

Prediction Uncertainty

We are interested in defining the expected uncertainty in the annual average dispersion estimates within the model domain for each year of the assessment period (1953–1989). The approach used in this assessment to define prediction uncertainty was to develop distributions of multiplicative correction factors that were applied to each concentration in the model domain. These multiplicative correction factors were developed from field validation data, joint frequency distribution comparisons, and parametric uncertainty analysis. Three components of uncertainty were evaluated:

1. Dispersion uncertainty
2. Meteorology uncertainty
3. Plume depletion uncertainty.

Dispersion uncertainty considers the uncertainty in predicting the annual average concentration of an inert, non-reactive tracer for a specific year, assuming we have the meteorological data for that year. Meteorology uncertainty arises because we are using 5-years of

meteorological data spanning a recent time period (1989–1993) to calculate an annual average X/Q value (concentration divided by release rate) that will be applied to all previous years (1953–1989) of the assessment period. Uncertainty in plume depletion via dry deposition was considered separately because dispersion uncertainty was based on tracer studies that typically employ inert, non-reactive tracers that have dry deposition velocities that are small and inconsequential. Uncertainty in plume depletion from wet deposition was not considered.

Dispersion Uncertainty. Dispersion uncertainty includes two sources: (1) errors in model input and (2) errors in model formulation or in the model itself (i.e., does the model adequately represent the physical process and phenomena it attempts to simulate). For example, suppose we select a location in the model domain and measure the concentration of tracer released from the site for an entire year. Let us assume the uncertainty associated with the measurement is small and inconsequential. Using the meteorological data recorded for that year, we calculate a concentration at the same receptor location using an appropriate atmospheric dispersion model. Assuming our model adequately represents the physical process and phenomena (i.e., if we had the correct inputs to the model, the output would match the observations), the uncertainty associated with the model prediction results from a lack of knowledge about the correct inputs to our model. Propagating these of uncertainties through the model calculation provides a distribution of model output. This is termed parameter uncertainty. The output distribution may be compared with measured data to see if model predictions encompass the measurements. Generally, agreement between predictions and observations is achieved when the model adequately represents the processes it attempts to simulate and choices regarding input parameter values have been made correctly.

Model uncertainty arises from the fact that perfect models cannot be constructed, and models often fail to adequately represent the physical process they attempt to simulate. In atmospheric dispersion models, the advection-dispersion process is often oversimplified and meteorological data required to characterize turbulence in the environment are lacking. In our previous example, the parameter uncertainty may not account for all differences between model predictions with observations if our model does not perfectly represent the physical process. Field validation exercises provide some information as to the overall performance of a model and in turn, model uncertainty. However, these are only partially relevant because field tests are generally not conducted under the same conditions that actual releases occurred.

The RATCHET model incorporates modules to explicitly assess parameter uncertainty. These parameters include wind direction, wind speed, atmospheric stability class, Monin-Obukhov length, precipitation rate, and mixing-layer depths. Other parameters may be assessed by simply varying the input according to some predefined distribution and repeating the simulation a number of times until an adequate output distribution is achieved. These methods are both time consuming and computationally intensive and fail to capture model uncertainty. In our approach, we ignored the built-in parameter uncertainty in RATCHET and focused our efforts on defining the distribution of a correction factor that will be applied to model output. (Parameter uncertainty was only used to evaluate uncertainty in plume depletion and deposition.) The correction factor was based on field experiments, considering the relevance of the experiment to actual release conditions and model domain environs. In this approach, we have ignored the mass balance features of RATCHET and have instead, treated the model output like that of a straight-line Gaussian Plume model, the only difference being that plume trajectories are not limited to straight lines.

We begin the process of defining the distribution of the correction factor for dispersion uncertainty by reviewing some field studies considered relevant to the assessment question (Table 6) which is what is the annual average concentration for each year of the assessment period. The correction factor is defined as the inverse of the distribution of predicted-to-observed ratios [$1/(C_p/C_o)$]. Relevant field studies included a model evaluation using the Rocky Flats Winter Validation Tracer Study data set (Rood 1999), validation exercises for RATCHET performed at the Hanford Reservation (Ramsdell et al. 1994), summaries of model validations performed for the Gaussian plume model (Miller and Hively 1987), and other studies reported in the literature. No one study is entirely relevant. Averaging times, release conditions, meteorological conditions, and terrain conditions are different than what we are attempting to simulate in this study. Nevertheless, these are the data we have chosen to work with and it is unlikely we will find a field validation experiment that was conducted under the exact conditions of past releases at Rocky Flats. Uncertainty bounds may be expanded to compensate for our lack of knowledge.

An additional study (Carhart et al. 1989) not reported in Table 6 included puff dispersion models that were similar to RATCHET (MESOPUFF, MESOPLUME). Evaluations were performed using tracer data bases from Oklahoma and the Savannah River Site. Oklahoma data consisted of two experiments measured at 100 and 600-km arcs downwind of a 3-hour perfluorocarbon release. The Savannah River data involved 15 separate experiments, 2 to 5 days in duration, where ^{85}Kr was released from a 61-m stack and measured at points 28 to 144-km downwind from the source. The ratio of the *average* predicted concentration to the *average* observed concentration was between 0.5 and 2. Note that this measure is different from the distribution of individual predicted-to-observed ratios reported in Table 6. There was also a tendency for models to overpredict concentrations in both data sets.

The study considered most relevant to the assessment question involved the RATCHET model using the Winter Validation Tracer Study data set. While it is true the release conditions for this study differed from those modeled (i.e., point source and area and elevated source) and the averaging time differed (i.e., annual average as opposed to 9-hour average), these data were obtained in the same environs that we are attempting to simulate. In addition, impacts on predicted and observed concentrations because of specific release conditions tend to diminish with increasing receptor distance. Release heights for Building 776 releases are not that much different from the Winter Validation Tracer Study in which the tracer was released at 10 m above ground level. Abbott and Rood (1996) also showed that the difference between a point and a 100-m diameter area source (represented by a series of point sources distributed in a circular area) released from a height of 0–19 m is at most 5% along the plume centerline at a distance of 2 km or greater for all combinations of wind speed and stability.

Building 771 stack releases differ from the Winter Validation Tracer Study releases mainly by the release height. Wind speed varies with height above the ground surface and is accounted for in the model. However, uncertainty exits in extrapolating wind speeds measured near the surface to elevated points. We conclude that the major difference between the Winter Validation Data set and our current situation resides with the averaging time and release height.

Table 6. Geometric Mean and Geometric Standard Deviation of Predicted-to-Observed Ratios for Field Studies Relevant to Defining the Correction Factor for Annual Average Concentrations

Model	Averaging time	Receptor distance	Release height	Environment	GM	GSD	Comments
RATCHET[a]	9-hour	8 km	10 m	complex terrain	0.86	4.4	Rocky Flats Winter Validation Study
RATCHET[a]	9-hour	16 km	10 m	complex terrain	1.1	4.3	Rocky Flats Winter Validation Study
RATCHET[b]	28-day	20–80 km	61 m	flat	1.4	2.2	Conducted at the Hanford Reservation
Gaussian Plume[c]	short-term	10 km	ground level	flat - highly instrumented		1.1	P/O ratios ranged from 0.8 to 1.2
Gaussian Plume[c]	short-term	10 km	elevated	flat - highly instrumented		1.2	P/O ratios ranged from 0.65 to 1.4
Gaussian Plume[c]	short -term	—	—	complex terrain		14	P/O ratios ranged from 0.01 to 100
Gaussian Plume[c]	annual average	—	—	complex terrain		3.8	P/O ratios ranged from 0.1 to 10
Gaussian Plume[c]	annual average	10 km	ground-level	flat		1.5	P/O ratios ranged from 0.5 to 2
Gaussian Plume[c]	annual average	10–50 km	ground-level	flat		2.2	P/O Ratios ranged from 0.25 to 4
Gaussian Plume[d]	12-hour	1–5 km	60 m	relatively flat	0.82	3.4	Terrain heights varied by about 50 m
Gaussian Plume[d]	72-hour	1–5 km	60 m	relatively flat	0.67	2.1	Terrain heights varied by about 50 m
Eulerian and Gaussian Plume[e]	annual average	1–1,000 km	0–60 m	relatively flat	0.75	1.5	Gaussian model used for receptors out to 50 km
CTDMPLUS[f]	12 to 72 hour	1 km	—	complex terrain	1.6	2.5	EPA complex terrain model

[a] Rood (1999).

[b] Ramsdell et al. (1994).

[c] Miller and Hively (1987).

[d] Robertson and Barry (1989).

[e] Simpson et al. (1990).

[f] Genikhovich and Schiermeier (1995).

The largest range of predicted-to-observed ratios reported in Table 6 involved complex terrain, which suggests models are more sensitive to the local meteorological and terrain conditions than other factors such as release height. For example, note the GSD for short-term estimates using the Gaussian plume model at a highly instrumented site for elevated source increases by about 9% from its ground-level counterpart but the difference between the GSD for flat and complex terrain is almost an order of magnitude.

With the distribution of predicted-to-observed ratios for RATCHET from the Winter Validation Tracer Study as our starting point, our approach was to modify this distribution based

(a) on the differences between the study conditions and those of past releases and (b) our assessment question (i.e. What is the annual average concentration for each year of the assessment period?). We combined data points at the 8 and 16-km distance into a composite set and justified this action based on the evaluations in Rood (1999) that showed similar GM and GSD values for 8 and 16-km data. In addition, the confidence intervals on the GM and variance of the observed-to-predicted ratio overlapped. The composite distribution had a GM of 0.95 and GSD of 4.4. Predicted to observed ratios are plotted as a function of the number of standard deviations from the mean (normalized to the standard normal distribution) in Figure 6. Note that most of the data points ($\pm 2\sigma$) lie along the line representing the lognormal fit to the data, with the exception of the tails. We, therefore, represent the distribution of predicted-to-observed ratios as a lognormal distribution with a GM and GSD as defined above. Points on the tails, particularly those with predicted-to-observed ratios less than 0.01, were associated with Test 5 (February 9, 1991) at the 8-km arc in the east northeast–NE sector for the hours 16:00 to 18:00. All models performed poorly for this test. Concentrations in east northeast sector were grossly underestimated (greater than a factor of 10 difference) and the ground-level contaminant mass at 8 km was also underestimated. Models appeared to have difficulty responding to the transition from daytime to nighttime stability conditions. During the latter hours of the test and under predominately nighttime conditions (18:00–23:00), predicted concentrations showed better agreement with the observations.

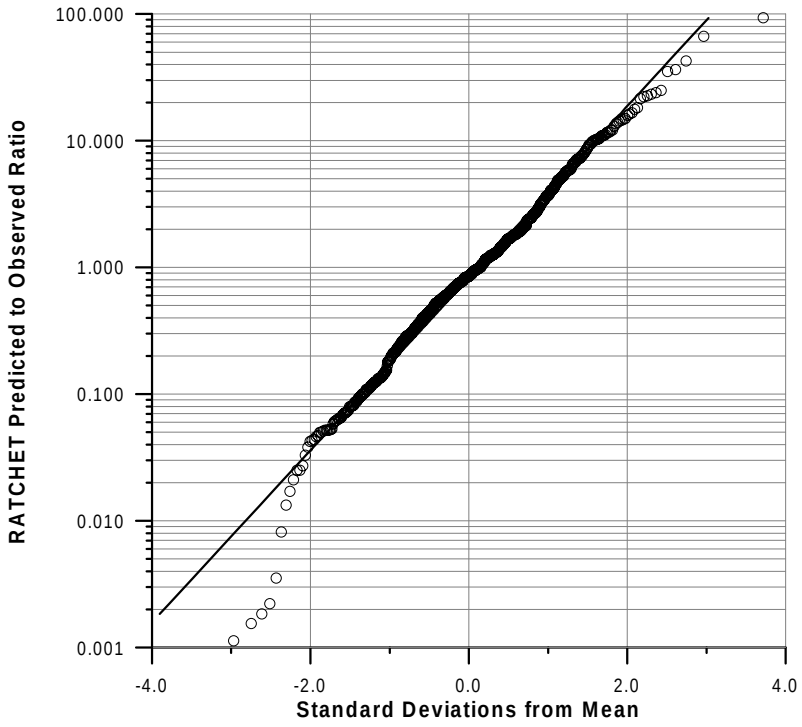

Figure 6. Predicted-to-observed ratios for the RATCHET model as a function of standard deviation from the mean (normalized to a mean of 0 and standard deviation of 1). The solid line represents the lognormal fit to the distribution. Circles represent individual data points.

As stated previously, the major difference between the Winter Validation Tracer Study data and the assessment question is the averaging time and release height. Averaging time appears to have a large impact on the range of predicted-to-observed ratios encountered. For example, Simpson et al. (1990) reports the GSD of the predicted-to-observed ratio is reduced 38% with an increase in averaging time from 12 to 72 hours (Table 6). Also note the GSD for the annual average and short-term predicted-to-observed ratio for the Gaussian plume model under complex terrain conditions increases from 3.8 to 14. Validation exercises performed with RATCHET at the Hanford Reservation for an elevated release at distances greater than 20 km showed a slight overprediction by the model (GM = 1.4) and a GSD value of 2.2, which is about 50% smaller than the GSD for the Winter Validation Tracer Study data. It is not clear whether these differences are due to averaging time, release height, terrain conditions, or receptor distance, but based on the other studies reviewed in Table 6, it is likely that the smaller GSD is primarily due to increased averaging time.

Key observations relevant to defining the distribution of the correction factor are summarized as follows:

- GSD of predicted-to-observed ratios decrease with increasing averaging time
- GSD of predicted-to-observed ratios increase with increasing terrain complexity
- GSD of predicted-to-observed ratios increase for receptor distances >10-km
- GM of the predicted-to-observed ratio is greater than 1.0 for receptor distances >20 km.

The GSD is expected to fall somewhere between 1.2 and 4.4 based on the data in Table 6. Noting the key observations stated above and the data in Table 6, the following values for GM and GSD were assigned to the predicted-to-observed ratio:

- GSD=2.2 and GM=0.95 for receptors <8 km
- GSD=2.0 and GM=0.95 for receptors >8 km and <16 km
- GSD=2.2 and GM=1.0 for receptors >16 km.

The distribution of predicted-to-observed ratios translate into dispersion correction factors listed in Table 8 in the summary section. The GSD value of 2.2 was the same value calculated for monthly averages using RATCHET at the Hanford Reservation. It may be argued that a lower value is more appropriate because the averaging time is longer. We have chosen this value because the GSD of monthly average predicted-to-observed ratios will likely be higher for Rocky Flats compared to Hanford because of terrain complexities. In addition, no annual average predicted-to-observed ratios exist for the Rocky Flats environs. Therefore, uncertainty bounds should be kept large to account for our lack of knowledge. Adjustments in the GSD and GM were also made to account for receptor distance. The GSD was reduced from 2.2 to 2.0 for receptors 8 to 16-km from RFP because the Winter Validation Tracer Study measurements were made at these distances and the lower value reflects our greater confidence in uncertainty at these distances. The GM was held at the same value calculated with the Winter Validation Tracer Study data for receptor distances <16 km and increased to 1.0 for receptor distances >16 km. The GM value was increased to reflect the tendency for models to overpredict at greater distances. Validation studies indicate predicted-to-observed ratios greater than 1.0 (reflecting model overprediction) at distances greater than 20 km. While this may be true, we have no site-specific data to verify this observation for our model domain. The lower GM predicted-to-observed value

will potentially result in model overprediction and, thereby, provide at least a conservative estimate of concentrations at these distances. Correction factor distributions were truncated by a minimum value of 0.01 and a maximum of 1000.

Application of this factor on a year-by-year basis assumes year-to-year annual average concentrations are independent from one another. Analysis of the annual average *X/Q* values for each year in the 5-year meteorological data set indicated annual average concentrations at some locations are correlated (to some degree) from year-to-year. Ideally, we would like to have meteorological data from the entire assessment period in order to estimate the year-to-year correlations, but these data are lacking. In order to account for the unknown year-to-year correlation, we have assumed a correlation coefficient of 1.0. This assumption will tend to overestimate uncertainty in time-integrated concentration (*TIC*), but is justified based on our lack of knowledge about year-to-year correlations. Details concerning incorporation of this factor in the Monte Carlo uncertainty analysis are discussed in the Risk Calculation section of this report.

Meteorology Uncertainty. Meteorology uncertainty arises because we are using 5 years of meteorological data spanning a recent time period (1989–1993) to define an annual average *X/Q* value (concentration divided by release rate) that will be applied to all previous years for the assessment period (1953–1989). The question is, how well does this 5-year period represent the past? Comparisons of annual average *X/Q* values computed with a 5-year data set to the annual average *X/Q* values computed using the meteorological data for each specific year was recently performed for the Fernald Dosimetry Reconstruction Project (Killough et al. 1998). Meteorological data from the Cincinnati Airport from 1987 to 1991 composed the 5-year composite meteorological data set. Annual average *X/Q* values computed with these data were then compared with the annual average *X/Q* value computed for each specific year using the meteorological data for that specific year. The years spanned from 1951 to 1991. Concentrations were calculated at 160 receptors ranging in distance from 1,000 to 10,000 m from the release point. A straight line Gaussian plume model for a 10-m release height was used to generate the *X /Q* values. The 5-year composite *X/Q* divided by the *X/Q* for the specific year (P/O ratio) forms the basis of the upper graph in Figure 7. A similar procedure was applied to the *X/Q* values generated for this study and is depicted in the lower graph in Figure 7. However, only the composite period is shown because meteorological data from previous years were not obtained. The lower graph in Figure 7 was generated using the RATCHET model and Building 776 *X/Q* values for 2,300 receptors in the model domain Figure 7 depicts the 5^{th}, 50^{th} and 95^{th} percentile of the cumulative frequency distribution for all points in the model domain. Note that for the composite period, the spread of the data is similar for both data sets.

As one would expect, the spread is much larger for those years that do not include the 5-year composite data. The long-term trend of these data may not depend strongly on location. If this procedure is applied to the RFP environs using Denver Stapleton International Airport data for instance, the locus of the 50^{th} percentiles is likely to look somewhat different, although the amplitudes may be similar. Obtaining meteorological data from past years (1953–1989) for Denver Stapleton International Airport and performing the calculations is not a trivial task, and the overall impact on the results may be similar to what is observed at Cincinnati based on a similar spread of these data for the composite period at both locations. For this reason, we have chosen instead to adapt these data to our analysis.

The Fernald data were represented by a multiplicative correction factor having a GM of 1.0 and GSD of 1.7. This distribution was developed using the following sampling scheme:

1. Noting from Figure 7 that the maximum range in the GMs is a factor of two, a GM was randomly selected from a log-uniform distribution with a minimum $2^{-1/2}$ and maximum $2^{-1/2}$.
2. Using the GM from step (1) and GSD = 1.61 (the maximum GSD calculated from the ratio of the 5-year composite *X/Q* to specific year *X/Q* for the 40 years of data), a sample is drawn from a lognormal distribution with these parameters.
3. Values are stored from step (2) and the process is repeated.

This somewhat conservative procedure takes account of the year-to-year variability in the GM of the 5-year composite *X/Q* to specific year *X/Q* ratio, as well as the uncertainty associated with distance and direction from the source. For a sample size of 1,000, a lognormal distribution was fitted with a GM = 1.0 and GSD = 1.7.

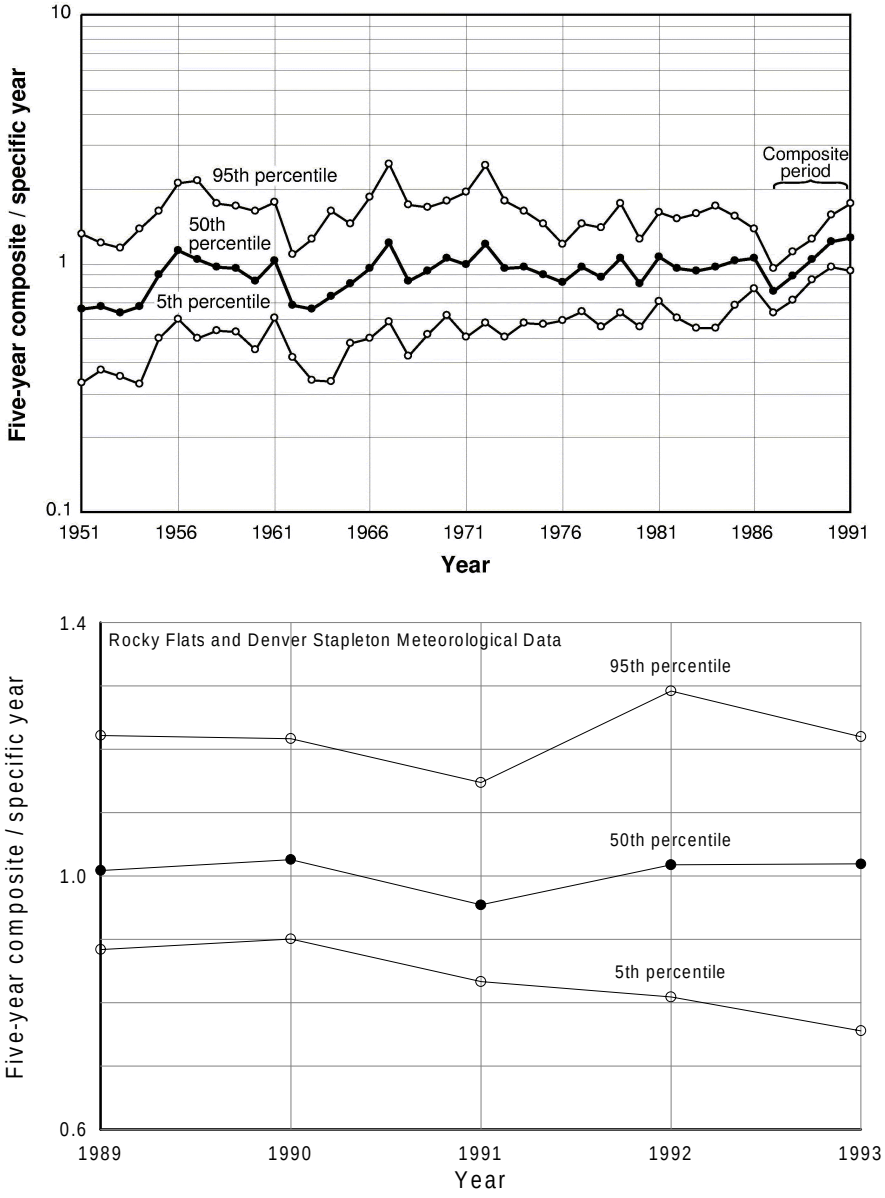

Figure 7. Distributions of P/O ratios for *X/Q* calculated with the Cincinnati meteorological data (upper graph) and RFP–Denver Stapleton International Airport meteorological data (lower graph). Predicted (P) corresponds to *X/Q* values for a five-year composite; observed (O) corresponds to the *X/Q* values for a specific year (from Killough et al. 1998).

Plume Depletion Uncertainty. One factor not considered in many of the field studies was plume depletion from dry deposition. Most field studies use inert tracers to avoid additional complications involving plume depletion and deposition. Miller et al. (1978) illustrates that plume depletion via dry deposition has little impact on inhalation dose for deposition velocities

less than 1.0 cm s^{-1} and release heights greater than 50 m for receptors within 10 km of the release point. For ground-level releases, plume depletion has a greater effect. The ratio of the depleted to nondepleted plume was 0.02 for deposition velocities in the 1.0 cm s^{-1} range and 0.67 for deposition velocities in the 0.1 cm s^{-1} range. Deposition velocities calculated in RATCHET ranged from 0.3 to 1.0 cm s^{-1}. Therefore, the actual amount of plume depletion would be somewhere between these values. Deposition velocities in the 1.0 cm s^{-1} range are associated with roughness lengths of around 2.0 m, which are limited to the foothills region of the model domain where few receptors are present. For these reasons, the uncertainty in the predicted concentration from plume depletion and deposition is expected to be small for most receptors in the model domain.

Deposition velocity is not an input parameter in RATCHET, but is calculated (using Equations 1–4) for each hour of the simulation. Deposition velocity is a function of the frictional velocity, wind speed, and a user-defined transfer resistance (r_t). The frictional velocity (Equation 4) is a function of wind speed, roughness height, and a stability correction factor that is a function of the Monin-Obukhov length and wind speed measurement height. Our approach is to vary the Monin-Obukhov length and transfer resistance and calculate alternative values for deposition velocity for a given wind speed and stability classification. Airborne concentrations calculated with alternative values for deposition velocity are compared to the airborne concentrations of the base case. The base case concentrations represent model predictions made using a transfer resistance of 100 s m^{-1} and a Monin-Obukhov length that represents the mid-range of possible values for a given stability class. (RATCHET uses the mid-range of the possible Monin-Obukhov lengths for a given stability class when run in a deterministic mode.)

The random sampling feature in RATCHET was used to vary the Monin-Obukhov length. When random sampling is selected, specific values of the inverse Monin-Obukhov length are obtained from the range of Monin-Obukhov lengths for a given stability class. A random value between 0 and 1 is obtained and used to calculate a value of the inverse Monin-Obukhov length assuming that the inverse Monin-Obukhov length is uniformly distributed within the range.

Distributions of the transfer resistance must be provided outside the RATCHET code. The rational for the distribution of r_t was based the distribution of deposition velocities reported in Harper et al. (1995). The 5^{th}, 50^{th}, and 95^{th} percentile values for deposition velocity for 1 μm particles and 5 m s^{-1} wind speed were 0.01, 0.21 and 4.1 cm s^{-1}, respectively. Assuming a lognormal distribution and a 50^{th} percentile r_t value of 100 s m^{-1}, we multiply the ratio of the $5^{th}/50^{th}$ percentile and $95^{th}/50^{th}$ percentile from the distribution of deposition velocities by the 50^{th} percentile transfer resistance value. The 5^{th} percentile for the distribution of r_t was $0.01/0.21 \times 100$ s m^{-1} = 4.8 s m^{-1}. The 95^{th} percentile for the distribution of r_t was $4.1/0.21 \times 100$ s m^{-1} = 1952 s m^{-1}. A lognormal distribution containing 200 individual r_t values was generated in Crystal Ball (Decisioneering 1996) and output to an ASCII file to be used in the uncertainty simulation. The corresponding 5^{th} and 95^{th} percentile deposition velocity calculated using a 5 m s^{-1} wind speed, roughness lengths from 0.001 to 2.0 m, and the mid-range value for the Monin-Obukhov length, was 0.05 and 1.5 cm s^{-1}, respectively. The range of deposition velocities used in plume depletion uncertainty simulations would be greater because the Monin-Obukhov length is also varied.

A shell program was written to facilitate the plume depletion uncertainty calculations. For each trial, a value of r_t was read from the distribution file created earlier, and written to the RATCHET input file. The RATCHET code was then called from the shell program and run

using meteorological data spanning 1 year (1990) and a unit release rate. Concentrations were output for 156 receptors located 1 to 32 km from the source. Output concentrations were saved and the process was repeated until all 100 r_t values were run. A correction factor was calculated for each trial and each receptor. The correction factor is given by

$$CF_{i,j} = \frac{C_{i,j}}{Cb_j} \tag{10}$$

where
$CF_{i,j}$ = the correction factor for i^{th} trial and j^{th} receptor,
$C_{i,j}$ = the concentration calculated for the i^{th} trial and j^{th} receptor, and
Cb_j = the base case concentration for the j^{th} receptor.

Correction factors were segregated into bins according to receptor distance. The GM and GSD were then calculated for all CF values within a given bin (Table 7).

These data show a GM near 1.0 and a GSD that increases as a function of receptor distance. As expected, the uncertainty is small, especially near the source, but uncertainty increases at greater receptor distances. The plume depletion uncertainty correction factor was assigned a lognormal distribution with a GM of 1.0 and a GSD that varies with receptor distance as given in Table 7.

Table 7. Plume Depletion Uncertainty Correction Factors

Distance (km)	GM	GSD
4	0.99	1.05
8	1.00	1.09
12	1.01	1.12
16	1.00	1.14
20	1.00	1.16
24	1.00	1.17
28	1.01	1.18
32	1.01	1.18

Summary of Prediction Uncertainty. Three correction factors are applied to our model predictions. The first correction factor accounts for the uncertainty in an annual average concentration of a non-reactive, non-depleting tracer, assuming we have the meteorological data for the that year. The second correction factor accounts for the uncertainty associated with using a 5-year composite meteorological data set (1989–1993) to predict the annual average concentrations for years past (1953–1989). The third correction factor accounts for uncertainty in the dry deposition rate and resulting plume depletion for specific year. The three correction factors are independent of one another and are represented by lognormal distributions. The dispersion correction factor is assumed to be correlated from year to year (correlation coefficient = 1.0). The other correction factors are independent from year-to-year. Table 8 summarizes all

three correction factors. Integration of these stochastic factors into the *TIC* estimates is discussed in the Risk Calculations section of this report.

Table 8. Summary of Uncertainty Correction Factors Applied to Annual Average Concentration Predictions

Receptor distance (km)	Dispersion uncertainty		Meteorology uncertainty		Depletion uncertainty	
	GM[a]	GSD	GM	GSD	GM	GSD
<4	1.1	2.2	1.0	1.7	1.0	1.05
8	1.1	2.0	1.0	1.7	1.0	1.09
12	1.1	2.0	1.0	1.7	1.0	1.12
16	1.1	2.0	1.0	1.7	1.0	1.14
20	1.0	2.2	1.0	1.7	1.0	1.16
24	1.0	2.2	1.0	1.7	1.0	1.17
28	1.0	2.2	1.0	1.7	1.0	1.18
>32	1.0	2.2	1.0	1.7	1.0	1.18

[a] Dispersion uncertainty GM is the inverse of the GM of predicted-to-observed ratios.

Annual Average *X*/*Q* Values

The procedure and models described in the previous sections were used to calculate an annual average *X*/*Q* for all concentration grid nodes in the model domain. Grid node spacing for the concentration grid was set at 1,000 m. Annual average *X*/*Q* values were calculated separately for releases from Building 776 (Figure 8) and Building 771 stack (Figure 9). The annual average *X*/*Q* at each of the grid nodes for each year of meteorological data (1989–1993) were computed for a constant unit release (1 Ci s^{-1}) from each building. The five *X*/*Q* values at each grid node were then averaged to yield a 5-year composite annual average X/Q. Isopleth maps were generated using *X*/*Q* data gridded using the minimum curvature routine found in the Surfer® software (Golden Software Inc. 1996).

The dispersion patterns shown in Figures 8 and 9 are characterized by a east northeast trending ellipsoid shaped plume. Wind roses constructed using RFP data from 1984–1993 (DOE 1995) indicate the predominant wind direction to be from the west northwest. Higher concentration isopleths near the source trend mostly easterly; however, farther away from the source, concentration isopleths trend to the northeast. The northeast trend is believed to be due to the influence of the Platte River Valley and the diurnal pattern of upslope-downslope conditions that characterize the general air movement on the Colorado Front Range environs (Crow 1974). Downslope conditions typically occur during the evening hours and are characterized by drainage flow of cooler air from the foothills to the plains. Westerly winds predominate, but the direction may be altered by local topography. Upslope conditions are a result of daytime heating and typically result in easterly winds that prevail during the daylight hours with transition from upslope to downslope conditions occurring during the evening and transition from downslope to upslope occurring during the morning. During evening hours under stable conditions, cool air near the surface drains from the Denver metropolitan area down the Platte River Valley (which flows to the northeast) and out to the plains. During daylight hours and after surface heating has

eliminated the cooler surface layer, the downslope conditions cease. This is followed by a brief period of relatively calm winds, which in turn is followed by return of air up the valley or upslope conditions. Meteorological data at Denver Stapleton International Airport captures these transitions in the Platte River Valley that are reflected in the *X*/*Q* isopleth maps.

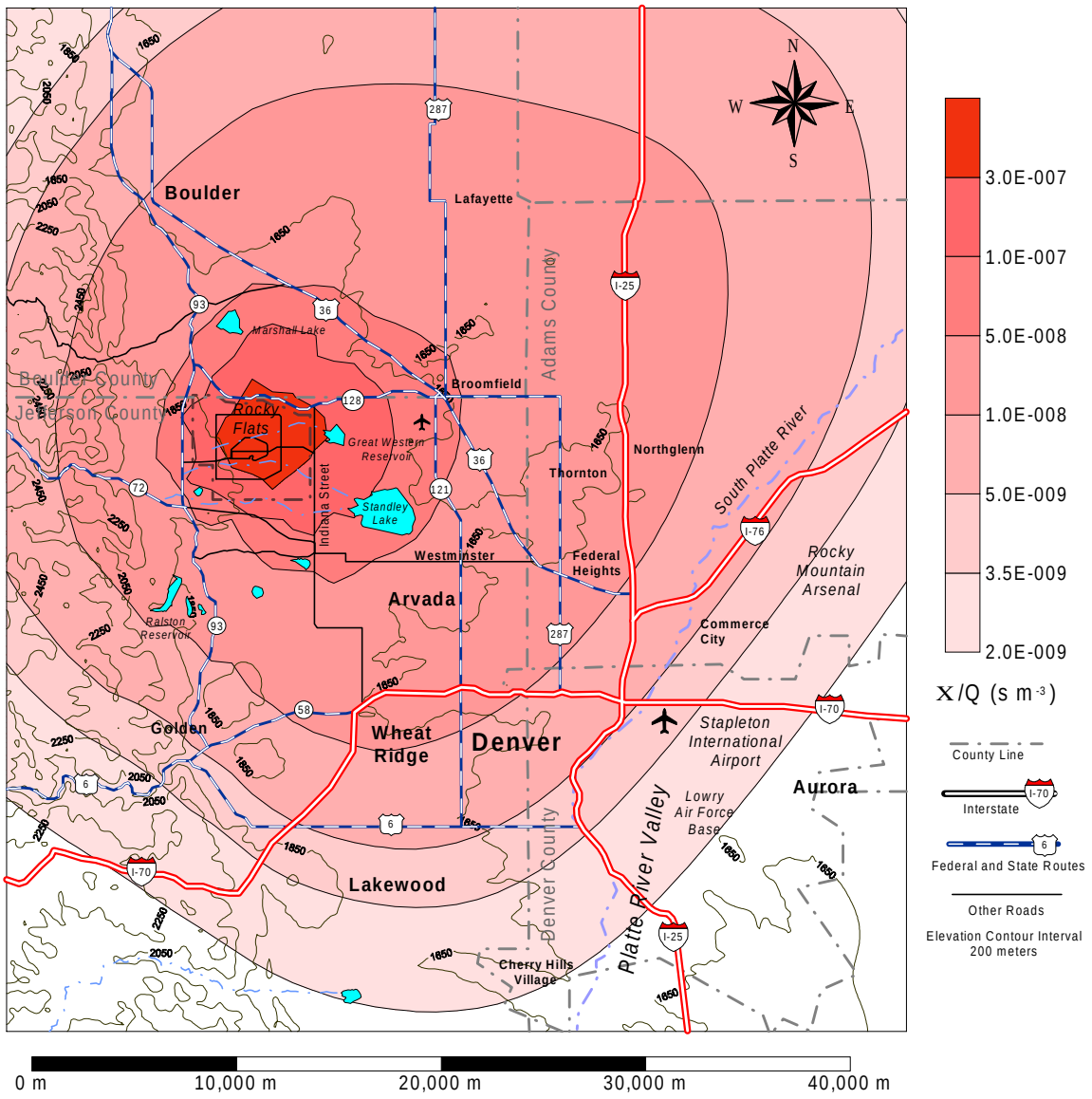

Figure 8. Isopleth map of the annual average X/Q for particulate releases from Building 776 using meteorological data from the RFP and Denver Stapleton Airport from 1989–1993.

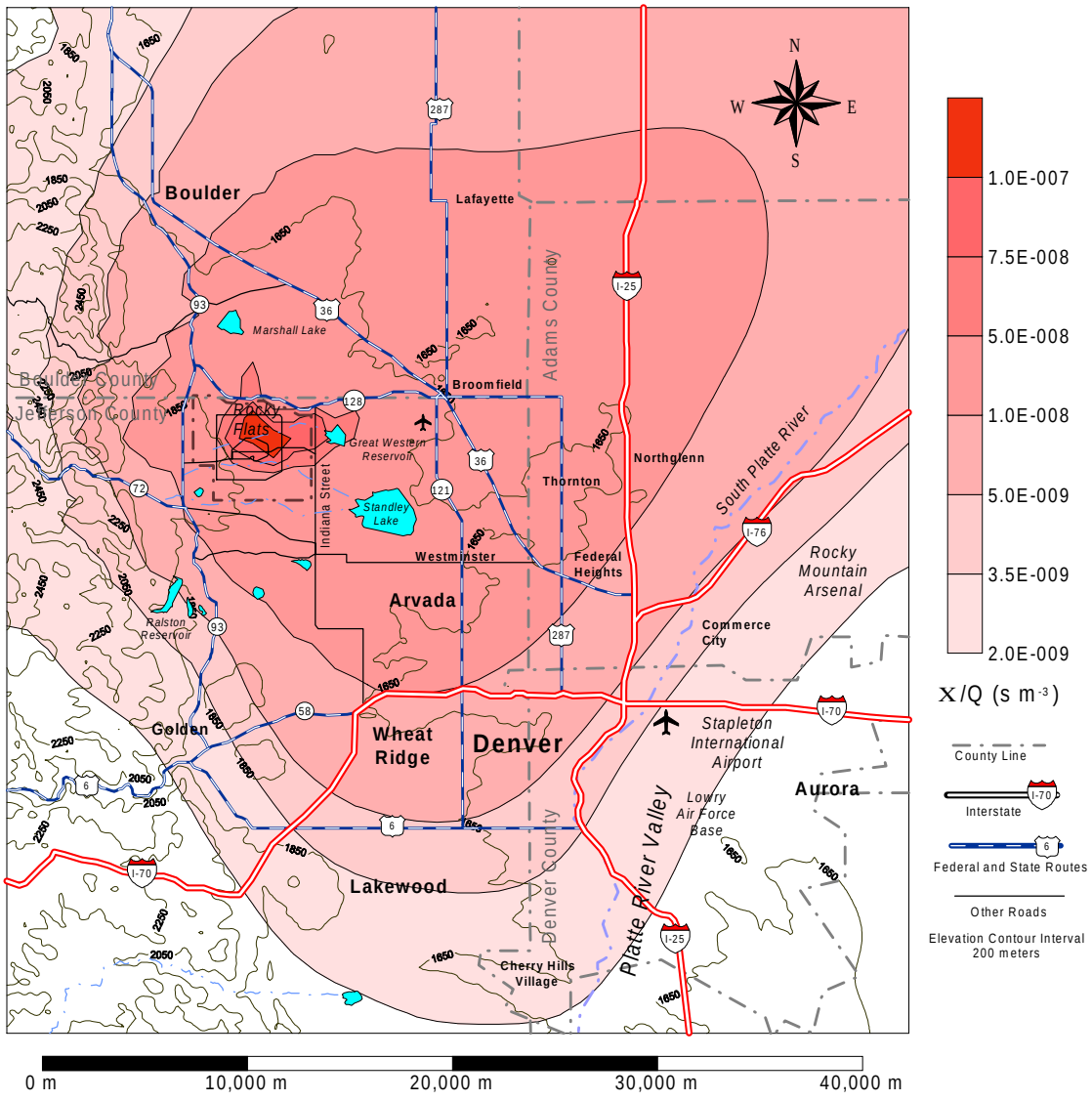

Figure 9. Isopleth map of the annual average X/Q for particulate releases from Building 771 using meteorological data from the RFP and Denver Stapleton Airport from 1989–1993.

Predicted Concentrations

Predicted concentrations of plutonium at specific receptors were calculated for each year in which source term information was available. Uncertainty in the predicted concentration included uncertainty in the dispersion estimate and source term. The concentration for the i^{th} year is given by

$$C_i = \sum_{j=1}^{2} \mathrm{X}/Q_j \; Q_{i,j} \; CF_1 \; CF_2 \; CF_3 \qquad (11)$$

where

X/Q_j = dispersion factor for source j (concentration divided by source term, y m^{-3}),
$Q_{i,j}$ = annual release of plutonium for the i^{th} year for j^{th} source (Building 776/777 or 771),
CF_1 = dispersion uncertainty correction factor,
CF_2 = meteorology uncertainty correction factor,
CF_3 = plume depletion uncertainty correction factor.

The correction factors and the source term (Q) are stochastic quantities. Therefore, the concentration is also stochastic quantity. The concentration a hypothetical receptor is exposed to is the sum of the prediction concentrations from Buildings 776/777 and 771 stack releases. Median value predicted concentrations at the location of highest concentration outside the buffer zone, which was east of the plant along Indiana Street, ranged from 4.5×10^{-5} fCi m^{-3} in 1978 to 1.0×10^{-1} fCi m^{-3} in 1957 (Figure 10).

For comparison, airborne concentrations of plutonium from nuclear weapons fallout (Rope et al. 1999) are also plotted in Figure 10. Note that predicted concentrations from normal operations are typically below concentrations from weapons fallout and only exceed for several years.

Time-integrated concentrations were calculated on a receptor-specific basis. Concentrations were integrated over the duration of time a receptor resided in a given location in the model domain and are reported in the Exposure Scenario and Risk Calculation section of the report.

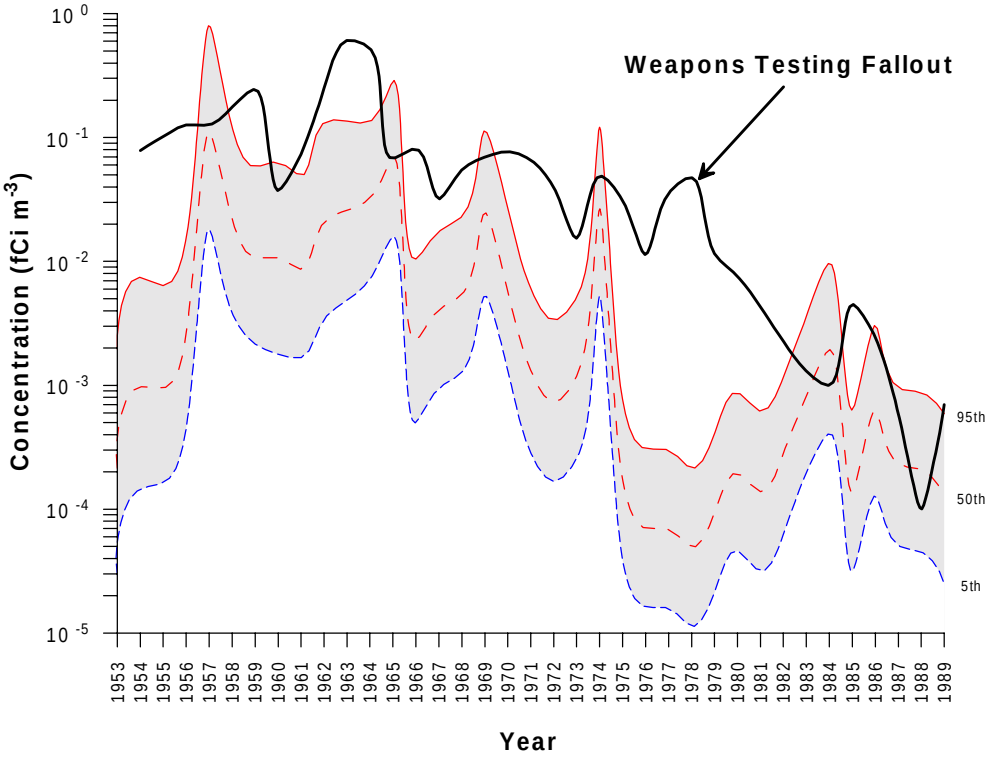

Figure 10. Predicted plutonium concentration as a function of year for a receptor located east of the plant on Indiana Street outside the current buffer zone. The heavy solid line identified as "Weapons testing fallout" represents estimated ^{239,240}Pu concentrations in fallout from nuclear weapons tests as reported in Rope et al. 1999.

EXPOSURE SCENARIOS AND RISK CALCULATIONS

One of the key parts of the Rocky Flats Dose Reconstruction work is calculating health impacts to people living in the surrounding area from materials released during RFP past operations. Dose reconstruction uses a pathways approach to study the potential radiation doses and health risks of these past releases on the surrounding communities. The pathways approach begins with learning what kinds of and how much materials were released from a facility and ends with estimating the health impacts these releases had on the residents in the area. Mathematical models described in the previous section were used to model the transport of materials released from the site to the surrounding communities. In this section, we calculate health impacts (incremental lifetime cancer incidence risk) to people living offsite from exposure to routine operational releases of plutonium.

The risk to a person from exposure to the plutonium released depends upon a number of factors, such as

- Lifestyle (that is, did the person spend a great deal of time outdoors or doing heavy work on a farm)
- When and how long that person lived near the RFP (for example, during the key release events in 1957 and late 1960s or in the 1970s when releases were less)
- Age and gender of the person
- Where the person lived and worked in relation to the RFP.

It is not realistic to calculate individual risks for every resident who may have lived or worked in the Rocky Flats area during its operational history. However it is also not credible to calculate a single risk that applies to all residents. To consider the many factors that influence exposure, we developed profiles, or exposure scenarios, of hypothetical, but realistic residents of the RFP area for which representative risk estimates could be made. Each scenario represents one individual. These scenarios incorporate typical lifestyles, ages, genders, and lengths of time in the area. The scenarios also specify and vary the home and work locations. These scenarios can help individuals determine risk ranges for themselves by finding a lifestyle profile that most closely matches their background. These scenarios are not designed to include all conceivable lifestyles of residents who lived in this region during the time of the RFP operations. Rather, they provide a range of potential profiles of people in the area.

We calculated risks from historical plutonium releases from the RFP for nine hypothetical exposure scenarios (Table 9). Inhalation was the only pathway of exposure considered in the assessment. Ingestion of plutonium in water and food and inhalation of plutonium deposited from routine operation and attached to soil are potential pathways that could have been considered in more detail. However, plutonium compounds are very insoluble and tend to adhere to soil making them relatively immobile and not readily taken up by plants or accumulating in the edible portions of animal products. Phase 1 results (ChemRisk 1994c) indicated inhalation to be the dominate pathway of exposure. For the later years (1980–1989) soil ingestion and inhalation of resuspended contaminated soil become a significant component of the total dose because of the accumulation and build up of deposited plutonium in soil and smaller airborne releases during this period. However, annual effective dose equivalents from pathways, other than direct inhalation for 1980–1989, are substantially lower than those for earlier time periods. Our

endpoint in this study is not annual effective dose equivalent but lifetime cancer incidence risk estimates from exposure to plutonium released from the RFP.

Exposure scenarios for the nine hypothetical receptors described in Table 9 were organized according to occupational and nonoccupational activities. Occupational activities include work, school, and extracurricular activities away from the home. Nonoccupational activities include time spent at home doing chores, sleeping, and leisure activities such as watching television. For some scenarios, the receptor was assumed to perform occupational and nonoccupational activities at a different location. For example, the office worker lived in Broomfield but worked in downtown Denver. The age of the receptor and years during which exposure occurred are also considered when calculating exposures. The last three exposure scenarios represent the same individual but at different periods in their life. Cumulative risks over this receptor's lifetime are also reported.

Table 9. Exposure Scenario Descriptions

Exposure scenario	Sex	Year of birth	Year beginning exposure	Year ending exposure	Location of occupational activities	Location of nonoccupational activities
Rancher	Male	1925	1953	1989	Indiana St.	Indiana St.
Office worker	Female	1951	1975	1989	Denver	Broomfield
Housewife	Female	1928	1953	1989	Broomfield	Broomfield
Retiree	Male	1923	1978	1989	Arvada	Arvada
Laborer #1	Male	1953	1974	1989	Thornton	Commerce City
Laborer #2	Male	1933	1953	1974	Commerce City	Westminster
Infant[a]	Female	1953	1953	1954	Broomfield	Broomfield
Child[a]	Female	1953	1955	1960	Broomfield	Broomfield
Student[a]	Female	1953	1961	1971	Westminster	Broomfield

[a] These receptors are the same individual. Cumulative risk over their lifetime is also reported

Breathing Rates and Time Budgets

Each exposure scenario was divided into three types of activities: sleeping, nonoccupational activity, and occupational activity. For the infant and child scenario, occupational and nonoccupational activities are irrelevant, so instead, activities were divided into sleeping and two other activities based on the child's age. For the infant, the other two activities were awake sedentary and awake active. For the child scenario, the two other activities were time spent at home (indoors and outdoors) and at preschool and/or day care.

For each activity, time spent at four different exercise levels was assigned. These exercise levels were resting, sitting (sedentary), light exercise, and heavy exercise. Some examples of light exercise are laboratory work, woodworking, housecleaning, and painting. Heavy exercise corresponds to occupations such as mining, construction, farming, and ranching. For each exercise level, an age- and gender-specific breathing rate was assigned. Breathing rates (Table 10) for persons age 8 and higher were obtained from Roy and Courtay (1991) and for children age 0–7 from Layton (1993).

Table 10. Breathing Rates for Various Exercise Levels as Reported in Roy and Courtay (1991) and Layton (1993)

Gender	Age	Resting ($m^3\ h^{-1}$)	Sitting ($m^3\ h^{-1}$)	Light ($m^3\ h^{-1}$)	Heavy ($m^3\ h^{-1}$)
Male	30-60	0.45	0.54	1.50	3.00
Female	30-60	0.32	0.39	1.26	2.70
Male	18	0.50	0.60	1.58	3.06
Female	18	0.35	0.42	1.32	1.44
Male	16	0.43	0.52	1.52	3.02
Female	16	0.35	0.42	1.30	2.70
Male	15	0.42	0.48	1.38	2.92
Female	15	0.35	0.40	1.30	2.57
Male	14	0.41	0.49	1.40	2.71
Female	14	0.33	0.40	1.20	2.52
Male	12	0.38	0.47	1.23	2.42
Female	12	0.33	0.39	1.13	2.17
Male	10	0.31	0.38	1.12	2.22
Female	10	0.31	0.38	1.12	1.84
Male	8	0.29	0.39	1.02	1.68
Female	8	0.29	0.39	1.02	1.68
Male	3-7	0.24	0.29	0.72	1.68
Female	3-7	0.23	0.27	0.68	1.59
Male	0-3	0.19	0.23	0.58	1.35
Female	0-3	0.14	0.17	0.45	1.02
Average, male[a]	8–17	0.37	0.45	1.28	1.49
Average, female[a]	8–17	0.33	0.40	1.18	2.25

[a] The average female breathing rate from age 8–17 was used in Scenario 9

Time budgets for various receptor activities were also based on Roy and Courtay (1991) (Table 11), but they were modified to fit specific exposure scenarios. The fraction of time spent at a specific exercise level while engaged in a given activity was assigned based on the nature of the activity. For example, the fraction of time spent at the resting exercise level while the receptor slept would be 1.0 and the other exercise levels would be 0. A weighted-average breathing rate was then applied to each activity based on the number of hours spent at each exercise level. For some scenarios (housewife, retiree, and laborer), nonoccupational activities were separated into those performed indoors and those performed outdoors. Although no distinction was made between indoor and outdoor air concentrations, exercise levels for indoor and outdoor activities differed. A time-weighted average breathing rate that included indoor and outdoor activities was calculated and applied to nonoccupational time. Each receptor was assumed to spend 15 days per year away from the Denver metropolitan area and outside the model domain. Contaminant concentrations were assumed to be the same for indoor and outdoor air.

Table 11. Time Budgets and Weighted Breathing Rates for the Exposure Scenarios

Scenario	Activity	Fraction of time spent at an exercise level				Hours per day (workweek)	Hours per day (weekend)	Hours per year	Weighted breathing rate ($m^3\ h^{-1}$)
		Resting	Sitting	Light	Heavy				
Rancher	Occupational	0.00	0.00	0.25	0.75	8.0	8.0	2800	2.62
	Nonoccupational	0.00	0.50	0.38	0.13	8.0	8.0	2800	1.21
	Sleeping	1.00	0.00	0.00	0.00	8.0	8.0	2800	0.45
Office worker	Occupational	0.00	0.25	0.75	0.00	8.0	0.0	2000	1.04
	Nonoccupational	0.00	0.50	0.38	0.13	8.0	16.0	3600	1.00
	Sleeping	1.00	0.00	0.00	0.00	8.0	8.0	2800	0.32
Housewife	Occupational	0.00	0.13	0.75	0.13	8.0	8.0	2800	1.33
	Nonoccupational								
	Indoor	0.00	0.50	0.38	0.13	4.0	4.0	1400	1.00
	Outdoor	0.00	0.38	0.50	0.13	4.0	4.0	1400	1.11
	Total nonoccupational	0.00	0.44	0.44	0.13	8.0	8.0	2800	1.06
	Sleeping	1.00	0.00	0.00	0.00	8.0	8.0	2800	0.32
Retiree	Occupational	0.00	0.50	0.50	0.00	8.0	8.0	2800	1.02
	Nonoccupational								
	Indoor	0.00	0.50	0.38	0.13	6.0	6.0	2100	1.21
	Outdoor	0.00	0.50	0.38	0.13	2.0	2.0	700	1.21
	Total nonoccupational	0.00	0.50	0.38	0.13			2800	1.21
	Sleeping	1.00	0.00	0.00	0.00	8.0	8.0	2800	0.45
Laborer #1	Occupational	0.00	0.13	0.50	0.38	8.0	0.0	2000	1.94
	Nonoccupational								
	Indoor	0.00	0.50	0.38	0.13	6.0	8.0	2300	1.21
	Outdoor	0.00	0.50	0.25	0.25	2.0	8.0	1300	1.40
	Total nonoccupational	0.00	0.50	0.31	0.19			3600	1.28
	Sleeping	1.00	0.00	0.00	0.00	8.0	8.0	2800	0.45
Laborer #2	Occupational	0.00	0.13	0.50	0.38	8.0	0.0	2000	1.94
	Nonoccupational								
	Indoor	0.00	0.50	0.38	0.13	6.0	8.0	2300	1.21
	Outdoor	0.00	0.50	0.25	0.25	2.0	8.0	1300	1.40
	Total nonoccupational	0.00	0.50	0.31	0.19			3600	1.28
	Sleeping	1.00	0.00	0.00	0.00	8.0	8.0	2800	0.45
Infant	Awake–sedentary	0.00	0.71	0.14	0.14	7.0	7.0	2450	0.33
	Awake –active	0.00	0.00	1.00	0.00	1.0	1.0	350	0.45
	Sleeping	1.00	0.00	0.00	0.00	16.0	16.0	5600	0.14
Child	Home								
	Indoor	0.00	0.50	0.42	0.08	6.0	6.0	2100	0.55
	Outdoor	0.00	0.00	0.67	0.33	1.5	1.5	525	1.04
	Total home					7.5	7.5	2625	0.65
	School-indoor	0.00	0.80	0.20	0.00	2.5	2.5	875	0.35
	Sleeping	1.00	0.00	0.00	0.00	14.0	14.0	4900	0.23
Student	Home								
	Indoor	0.00	0.44	0.56	0.00	4.5	8.0	1925	0.83
	Outdoor	0.00	0.00	0.25	0.75	2.5	6.0	1225	1.98
	Total home	0.00	0.22	0.40	0.38	7.0	14.0	3150	1.28
	School								
	Indoor	0.00	0.75	0.25	0.00	6.0	0.0	1500	0.59
	Outdoor	0.00	0.00	0.25	0.75	1.0	0.0	250	1.98
	Total school	0.00	0.38	0.25	0.38	7.0	0.0	1750	0.79
	Sleeping	1.00	0.00	0.00	0.00	10.0	10.0	3500	0.33

Time-weighted average breathing rates were calculated for the three activities for which each receptor was assumed to be engaged. The time-weighted average breathing rate is given by

$$WBR_j = \sum_{i=1}^{4} BR_i \; f_{i,j} \tag{12}$$

where

WBR_j = time-weighted average breathing rate for the j^{th} activity ($m^3\ h^{-1}$),
BR_i = breathing rate for the i^{th} exercise level ($m^3\ h^{-1}$),
$f_{i,j}$ = fraction of time spent at the i^{th} exercise level for the j^{th} activity.

To summarize, three activities were defined for each exposure scenario: sleeping, occupational, and nonoccupational. The location of exposure for occupational activities may be different from nonoccupational activities. Four different exercise levels, each with an assigned breathing rate, were distinguished: resting, sitting, light exercise, and heavy exercise. The breathing rate during a given activity was the time-weighted average breathing rate of the four exercise levels.

Risk Calculation and Uncertainty

The calculation of incremental lifetime cancer incidence risk involved three steps:

1. Calculate the *TIC* at the point of exposure.
2. Calculate the amount of plutonium inhaled by the receptor.
3. Multiply the plutonium intake by a risk coefficient that relates the incremental lifetime cancer incidence risk to the amount of plutonium inhaled.

In each step, Monte Carlo sampling techniques were used to propagate uncertainty through the calculation. A Monte Carlo calculation consists of multiple iterations or trials of a computational endpoint (risk). For each trial, parameter values are randomly chosen from distributions that quantitatively describe our knowledge of the parameter. After randomly selecting a set of parameter values, the endpoint is calculated and the procedure is repeated numerous times until an adequate distribution of the endpoint is obtained.

Uncertainty in risk estimates include uncertainty in the *TIC* and risk coefficients. Receptor behavior patterns (i.e., the time spent doing different activities at different exertion levels) and their physical attributes (body weight and breathing rate) were considered fixed quantities.

The procedure outlined above requires an estimate of the *TIC* at the point of exposure. A receptor can be exposed at two locations; place of work (occupational) and place of residence (nonoccupational and sleeping). Consider a Monte Carlo calculation consisting of m trials. The *TIC* of the k^{th} trial ($0 < k \leq m$) for source j and location i is

$$TIC_{i,j} = CF_1 \sum_{l=1}^{n} CF_2 \; CF_3 \; \mathrm{X}/Q_{i,j} \; Q_{j,l} \; \Delta t \tag{13}$$

where

$X/Q_{i,j}$ = dispersion factor for source j and location i ($y\ m^{-3}$),
$Q_{j,l}$ = source term for year l and source j ($\mu Ci\ y^{-1}$),

CF_1 = stochastic correction factor for dispersion (unitless),
CF_2 = stochastic correction factor meteorology (unitless),
CF_3 = stochastic correction factor for deposition and plume depletion (unitless),
n = number of years exposed,
Δt = time increment (1 year).

Notice that the dispersion correction factor (CF_1) is outside the summation symbol. For each Monte Carlo trial, CF_1 is sampled once but the correction factors, CF_2, CF_3, and source term are sampled n times. This sampling scheme was used to allow for year-to-year correlation in annual dispersion estimates as discussed earlier. The amount of plutonium inhaled by a receptor for the k^{th} Monte Carlo trial is

$$I = \sum_{j=1}^{2} \left(TIC_{1,j}\, WBR_1\, T_1 + TIC_{2,j}\, WBR_2\, T_2 + TIC_{2,j}\, WBR_3\, T_3 \right) \qquad (14)$$

where
I = intake of plutonium by the receptor for the exposure period (μCi),
$TIC_{1,2}j$ = time-integrated concentration for occupational and nonoccupational (including sleeping) locations and j^{th} source (μCi-y m^{-3}),
$WBR_{1,2,3}$ = time-weighted average breathing rate for occupational, nonoccupational, and sleeping activity (m^3 h^{-1}),
$T_{1,2,3}$ = hours per year for occupational, nonoccupational, and sleeping activity (h y^{-1}).

The subscripts 1, 2, 3 refer to occupational, nonoccupational, and sleeping activity respectively. Note that the *TIC* values (Table 12) are only calculated at 2 locations and that the same *TIC* value is applied to sleeping and nonoccupational awake activities.

Distributions of *TIC* values in Table 12 are described in terms of their *GM* and *GSD*. Analysis of the data points that comprise these distributions show they are best represented by a lognormal distribution. However, in practice, calculations are performed using the actual distribution (made up of *m* number of trials) and not the lognormal representation. Magnitude of the *TIC* was dependent on the length of exposure, location of exposure, and magnitude of source during exposure. Differences in the GSD values between scenarios are mainly related to the length of exposure and magnitude of the dispersion correction factor. Longer integration time typically corresponds to lower *GSD*s (but not lower variance) because summation of the independent stochastic variables (CF_2 and CF_3) over the integration period results in a lower coefficient of variation (*CV*) of the sum compared to the *CV* of individual years. The *CV* is the standard deviation of the sum divided by the mean of the sum (σ/μ). Like the *CV*, the GSD is a relative measure of the spread of the data comprising the distribution. The decrease in the GSD for longer averaging times is because the *relative* variability in the *TIC* decreases with increasing integration time.

Table 12. Time-Integrated Concentrations for Each Receptor Scenario and Source for Occupational and Nonoccupational Activities

Scenario	Activity	Time-integrated concentration, Building 444[a] (μCi-y m^{-3})	Time-integrated concentration, Building 776[a] (μCi-y m^{-3})
Rancher	Occupational	2.8×10^{-10} (2.5)	1.4×10^{-10} (2.3)
	Nonoccupational	2.8×10^{-10} (2.5)	1.4×10^{-10} (2.3)
Office worker	Occupational	3.9×10^{-14} (2.4)	4.8×10^{-14} (2.3)
	Nonoccupational	3.3×10^{-13} (2.1)	7.9×10^{-13} (2.1)
Housewife	Occupational	9.9×10^{-11} (2.3)	2.6×10^{-11} (2.1)
	Nonoccupational	9.9×10^{-11} (2.3)	2.6×10^{-11} (2.1)
Retiree	Occupational	1.5×10^{-13} (2.1)	2.4×10^{-13} (2.1)
	Nonoccupational	1.5×10^{-13} (2.1)	2.4×10^{-13} (2.1)
Laborer #1	Occupational	2.0×10^{-13} (2.1)	1.4×10^{-12} (2.3)
	Nonoccupational	5.7×10^{-14} (2.3)	4.8×10^{-13}(2.5)
Laborer #2	Occupational	1.5×10^{-11} (2.4)	2.3×10^{-12} (2.3)
	Nonoccupational	8.2×10^{-11} (2.2)	1.9×10^{-11} (2.1)
Infant	Occupational	4.5×10^{-13} (2.8)	4.1×10^{-19} (2.4)
	Nonoccupational	4.5×10^{-13} (2.8)	4.1×10^{-19} (2.4)
Child	Occupational	5.5×10^{-11} (2.5)	1.6×10^{-12} (2.7)
	Nonoccupational	5.2×10^{-11} (2.5)	1.6×10^{-12} (2.7)
Student	Occupational	3.1×10^{-11} (2.1)	1.3×10^{-11} (2.1)
	Nonoccupational	3.8×10^{-11} (2.1)	1.8×10^{-11} (2.1)

[a] Geometric mean (geometric standard deviation)

Calculating the lifetime cancer incidence risk requires estimates of risk coefficients for plutonium. Risk coefficients relate the lifetime risk of cancer incidence to the amount of plutonium inhaled. Plutonium risk coefficients were developed in Phase II of the study and are documented in Grogan et al. (1999).

Plutonium emits alpha particles that have such weak penetration abilities they can be blocked by a piece of paper or the dead, outer layers of the skin. As a result, the major danger from plutonium comes from having it inside the body. For residents in the vicinity of Rocky Flats, plutonium most likely entered the body from breathing air that contained plutonium particles released from the site. After inhalation, plutonium enters the blood and about 80% is transported to the bone or liver where it is retained for years. Following inhalation, the four most highly exposed tissues are bone surface, lung, liver, and bone marrow. These tissues account for more than 97% of the total dose received by infants and adults alike. The dose per unit activity inhaled varies for these four tissues (see Table 13). The particle size distribution of the inhaled plutonium aerosol was assumed to have an activity median aerodynamic diameter (AMAD) of 1 µm and a GSD of 2.5 (Table 13). This particle size distribution accounts for routine vent and stack effluents that were effectively filtered which result in aerosols with an AMAD of ~0.3 µm, and the larger particles that would have been released when filter leakage occurred. The inhaled plutonium is assumed to be in the oxide form.

Table 13. Plutonium Inhalation Dose Conversion Factors for a 1-µm AMAD Aerosol with a GSD of 2.5[a]

Cancer site	Dose conversion factor (µGy Bq^{-1}) [b]
Lung	4.4 (1.9)
Liver	2.0 (3.0)
Bone	9.0 (3.0)
Bone marrow	0.46 (3.0)

[a] ICRP 1995

[b] Geometric mean (geometric standard deviation).

The incidence of health effects depends on the amount of dose received. Two main classes of health effects are induced by ionizing radiation: deterministic and stochastic effects. Deterministic effects most often follow acute, high dose exposure. The severity of the effect increases with dose above the threshold dose. Below the threshold dose, the effect is not evident; however, subtle minor effects may occur. Deterministic effects cause direct damage to tissues and include effects that most often occur within days to weeks after exposure. For example, these effects can cause reddening of the skin, cataracts, hair loss, sterility, and bone marrow depression after external irradiation. After inhalation of plutonium, deterministic effects may include radiation pneumonitis, pulmonary fibrosis, and lymphopenia, but these conditions occur only after very high doses. The threshold dose for most deterministic effects is at least 0.5 Gy delivered in a short time, and many are much higher (NCRP 1991). For the releases of plutonium that occurred from the site, doses to individuals in the Rocky Flats area were well below the threshold doses. Therefore, deterministic health effects were not possible.

Stochastic effects are assumed to occur randomly at all dose levels, including the lowest doses. The frequency of stochastic effects is dependent on the dose, and the effects usually occur at long intervals after exposure. In a large population exposed to low doses, only a few of the exposed individuals will be affected, most will not. The two principal types of stochastic effects are induced cancer and genetic effects. For exposure to plutonium, the risk of induced cancer is the health effect of most concern; in particular, lung cancer, liver cancer, bone cancer, and leukemia (bone marrow exposure) because these are the tissues that receive the highest doses. Genetic effects are not an important risk for plutonium exposures because (a) people exposed to radiation are several times more likely to be affected by an induced cancer than to transmit genetic effects to their children and (b) the plutonium doses to the gonads (ovaries or testes) are small compared to other organs of the body (40 times less than the lung). Therefore, we did not consider them further.

The alpha particles emitted from plutonium are densely ionizing, and the linear energy transfer (LET) to the tissue is high over the short range (about 40 µm) of the alpha particles (thus, the name high-LET radiation). Other radiations, such as gamma rays and x-rays, are less densely ionizing and are termed low-LET radiations. The biological effects of low-LET radiation are better known than those of high-LET radiation. The differences between radiation types are important to the analysis because high-LET radiations are more biologically effective (cause more damage) per unit of dose than low-LET radiations. This difference in effectiveness is usually described by the relative biological effectiveness (RBE), which is the ratio of doses from two different radiations to produce the same type and level of biological effect.

Inhalation of plutonium results in the exposure of organs to high-LET radiation. While a few human populations have been exposed directly to large amounts of plutonium and some populations to other radionuclides that emit alpha particles, more groups have been exposed to low-LET gamma radiation and have been evaluated in more epidemiologic detail. In addition, studies of cancer in animals exposed to both types of radiation and laboratory studies of cellular and other biological endpoints can be used to support human studies. These different sources of information were used in this phase of the study to develop four independent approaches to estimate the risk of cancer because of radiation doses from plutonium deposited in the organs of the human body (Grogan et al. 1999). Three approaches used epidemiologic studies of human populations to derive dose-response relationships, and the fourth approach used dose-response relationships from controlled animal experiments. The four independent approaches were used to derive, where possible, risk coefficients for each organ of interest. The coefficients from the different approaches were then combined by weighting each according its intrinsic merit to produce a single risk coefficient with uncertainties for each organ of interest.

The influence of gender and age was accounted for in the analyses (see Grogan et al. [1999] for details). The data allowed a distinction to be made between the risks and uncertainties to those under 20 years of age at exposure and those 20 and older. The data did not warrant a more detailed analysis. For this reason, the risk coefficients for persons under 20 years of age were applied to the infants and children in the seven hypothetical exposure scenarios.

The GM (50^{th} percentile) and GSDs of the cancer incidence risk coefficient distributions are listed in Table 14. The units reported in Grogan et al. (1999) have been changed from risk per 100,000 persons per unit of activity in kilobecquerels (kBq) to risk per 10,000 persons per unit of activity in microcuries (µCi). These numbers indicate the median number of cases of cancer (fatal and nonfatal) that would be expected to result from 10,000 people all inhaling 1 µCi of ^{239,240}Pu particles with the defined particle size distribution. A 1-µm AMAD aerosol with a GSD of 2.5 was used to characterize the particle size distribution of the routine operational effluent.

Table 14. Lifetime Cancer Incidence Risk[a] Per 10,000 Persons per 1 µCi of Inhaled ^{239,240}Pu for 1-µm AMAD Particles (GSD=2.5) Used to Characterize Routine Releases

Cancer site	Gender	Age under 20	Age 20 and older
Lung	Male	206 (3.5)	210 (3.4)
	Female	206 (3.5)	210 (3.4)
Liver	Male	92 (5.2)	49 (5.2)
	Female	45 (5.4)	23 (5.4)
Bone	Male	16 (9.5)	8 (9.3)
	Female	8 (10)	4 (10)
Bone marrow	Male	2.4 (6.1)	2.3 (6.3)
	Female	2.4 (6.1)	2.3 (6.3)

[a] Geometric mean (geometric standard deviation).

The incremental lifetime cancer incidence risk is then calculated by multiplying the integrated plutonium intake (Equation 14) by the appropriate risk coefficient for each organ of concern.

Monte Carlo sampling was performed using a FORTRAN program written specifically for this application. Each step of the Monte Carlo simulation is described below:

1. The distribution of *TIC* values (Equation 13) for each receptor activity and each source were calculated first. Nonoccupational and sleeping activities were assumed to be at the same location. Therefore, 2 *TIC* values were calculated for each receptor and each source. Each *TIC* distribution contained *m* number of individual trials. If occupational and nonoccupational activities occurred at the same location, then a single *TIC* value was used for each source.
2. Each of the *TIC* trials are multiplied by the WBR_i and T_i, (corresponding to the i^{th} receptor activity), then summed over all sources and receptor activities to yield the total contaminant intake of the k^{th} trial (Equation 14). The procedure is repeated for all *m* trials
3. Each estimate of total contaminant intake is multiplied by a randomly selected risk coefficient to give an estimate of the incremental lifetime cancer incidence risk. This calculation is repeated *m* times to yield a distribution of lifetime cancer incidence risks.
4. Percentiles, GM, and GSD values were then calculated from the distribution of *m* risk values.

The total risk over the lifetime of the individual that represents the infant, child, and student scenarios was calculated differently. For each trial, contaminant intake was calculated for each year the receptor was exposed. Note that the breathing rate changes as the individual matures. Meteorological, deposition, and source term uncertainty were applied to each years intake estimate. Intakes were summed across all years of exposure then multiplied by the dispersion correction factor and the risk coefficient for persons under 20. This process was repeated *m* times resulting in a distribution of incremental lifetime cancer incidence risk estimates for the receptor.

FORTRAN routines for generating random numbers and selecting values from normal, lognormal, triangular, and uniform distributions were adapted from Press et al. (1992). The output distributions provided in this report were generated from 2,000 trials.

LIFETIME CANCER INCIDENCE RISK ESTIMATES

Incremental lifetime cancer incidence risk was greatest for the rancher scenario followed by the housewife, laborer #2, and total child scenarios depending on the organ of interest. Appendix A contains detailed output from the computer code used to calculate time-integrated concentrations and risk values. The organ with the greatest risk was the lung followed by the liver, bone, and bone marrow. Risk estimates were lognormally distributed and described by the GM and GSD for each scenario and organ of concern (Table 15). Geometric mean risk values for the lung varied from 1.1×10^{-7} for the rancher scenario to 1.6×10^{-11} for the infant. The 5^{th} and 95^{th} percentiles of the sum of the incremental lifetime cancer incidence risk across all organs are shown graphically in Figure 11. Using the rancher scenario and lung risk as an example, these risks may be interpreted as follows:

- There is a 90% probability that incremental lifetime carcinogenic incidence risk to the lung for the rancher was between 1.0×10^{-8} (5% value) and 2.1×10^{-6} (95% value).
- There is a 5% probability that incremental lifetime carcinogenic incidence risk to the lung for the rancher was greater than 2.1×10^{-6} and a 5% probability the risk was less than 1.0×10^{-8}.

Table 15. Lifetime Cancer Incidence Risk[a] for Lung, Liver, Bone Surface, and Bone Marrow Calculated for the Nine Exposure Scenarios

Scenario	Lung	Liver	Bone	Bone Marrow
Rancher	1.1×10^{-7} (4.6)	2.4×10^{-8} (6.4)	5.1×10^{-9} (12)	1.2×10^{-9} (5.1)
Office worker	1.1×10^{-10} (4.1)	1.2×10^{-11} (6.3)	2.5×10^{-12} (11)	1.2×10^{-12} (7.1)
Housewife	1.9×10^{-8} (4.6)	2.3×10^{-9} (6.8)	4.9×10^{-10} (11)	2.1×10^{-10} (7.2)
Retiree	6.2×10^{-11} (4.0)	1.4×10^{-11} (6.5)	2.9×10^{-12} (11)	6.9×10^{-13} (7.0)
Laborer #1	1.9×10^{-10} (4.6)	4.6×10^{-11} (6.3)	8.7×10^{-12} (12)	2.2×10^{-12} (7.4)
Laborer #2	1.3×10^{-8} (4.4)	3.1×10^{-9} (6.1)	6.4×10^{-9} (11)	1.6×10^{-10} (7.0)
Infant	1.6×10^{-11} (5.1)	3.5×10^{-12} (6.8)	7.3×10^{-13} (12)	1.8×10^{-13} (8.1)
Child	3.5×10^{-9} (5.0)	7.3×10^{-10} (7.0)	1.6×10^{-10} (13)	4.0×10^{-11} (8.1)
Student	6.8×10^{-9} (4.4)	1.5×10^{-9} (6.4)	3.3×10^{-10} (11)	7.9×10^{-11} (7.2)
Total (Child)	1.2×10^{-8} (4.2)	2.6×10^{-9} (6.3)	5.6×10^{-10} (12)	1.4×10^{-10} (6.7)

[a] Geometric mean (geometric standard deviation)

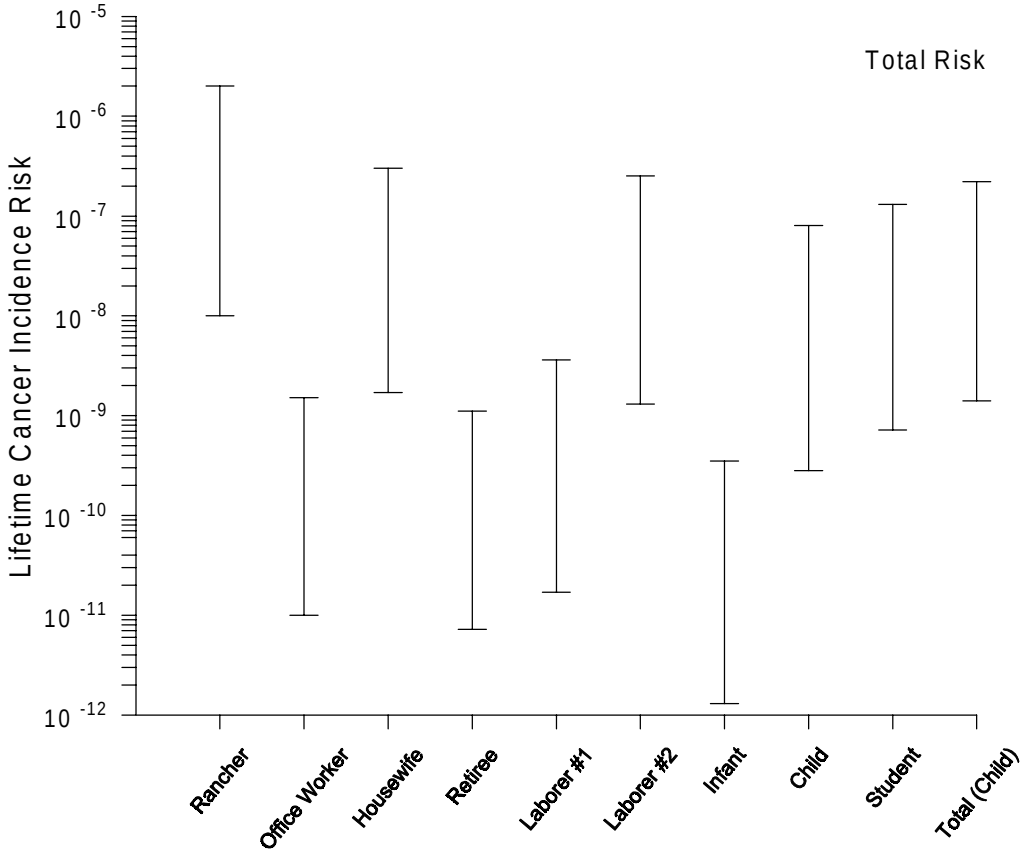

Figure 11. Incremental lifetime cancer incidence risk estimates for all organs (lung, liver, bone surface, and bone marrow) for the nine exposure scenarios. The range of values shown represent the 5th and 95th percentiles on the cumulative density function. The Total (Child) represents the sum of the infant, child, and student scenarios.

We may also interpret this to mean, given an exposure history and lifestyle similar to that of the rancher scenario, there is a 95% probability that the model-predicted number of lung cancer cases attributed to inhalation of plutonium originating from the RFP would be no greater than 2 persons in a population of 1 million similarly exposed individuals.

The magnitude of the lifetime risk was dependent on a number of factors, which included duration of exposure, year(s) when exposure occurred, location of exposure, and lifestyle of the receptor. The rancher and housewife scenario generally had the highest risks; this was primarily due to their close proximity to the RFP (Indiana Street and Broomfield, respectively) and their duration of exposure. The infant scenario had the lowest risk primarily because her duration of exposure was short (1 year) and releases for 1953 were smaller compared to releases in the late 50s and 60s. The infant and child scenarios typically exhibited the greatest variability as measured by the GSD. This variability was primarily due to uncertainty associated with the time-integrated concentration and source term (see Table 12).

Also note that the risks for the laborer #2 scenario are substantially higher than those for the laborer #1 scenario. Geometric mean lung risk for the laborer #1 scenario was 1.9×10^{-10} compared to 1.3×10^{-8} for the laborer #2 scenario. These differences are attributed to the years over which exposure occurred. The exposure period for the laborer #1 receptor was 1974–1989 while the exposure period for the laborer #2 receptor was 1953–1974. Releases during the earlier years of operation (late 50s and 60s) were higher than later years and, therefore, resulted in higher lifetime cancer incidence risks. Also note the difference between the risks for the laborer #1 scenario and the office worker scenario. Exposure time was approximately the same but risks for the laborer were slightly greater and showed greater variability. Several factors contributed to these differences. First, location and type of activity the receptor was engaged in differed (the laborer worked closer to the plant and exhibited higher breathing rates than the office worker). Second, the laborer was exposed to the high releases from Building 776 in 1974 (see Figure 2) while the office worker had not moved into the area at that time.

There are almost an infinite number of possible exposure scenarios that can be defined, and in most cases, the risks associated with each scenario will differ. However, the risks will probably be bounded by the risks associated with the rancher scenario. The scenario involving the rancher may be considered the maximum exposed individual in the model domain because he was placed at the point of highest concentration outside the RFP buffer zone and remained there for the entire operating period of the plant. However, it is recognized that ranchers could have been grazing cattle within the current buffer zone and up to the old cattle fence. There were also bunkhouses or some type of permanent overnight ranch camp to the northeast within the buffer zone. To increase the risk substantially from our estimates, the concentration within the buffer zone would have to be several orders of magnitude greater than outside it. This simply is not the case as is evidenced by the X/Q plots provided previously in the report. The resulting risk, accounting for occupancy time while exposed to concentrations within the buffer zone, would likely still be in the 10^{-7} to 10^{-6} range.

REFERENCES

Abbott, M.L. and A.S. Rood 1996. *Source Group Optimization Program (SGOP): A Program that Groups Emission Sources for Input into Air Dispersion Models.* INEL-96/0376. Idaho National Engineering Laboratory, Idaho Falls, Idaho.

Briggs, G.A. 1969. *Plume Rise.* TID-25075, U. S. Atomic Energy Commission, Washington D.C.

Briggs, G.A. 1975 "Plume Rise Predictions". Lectures on Air Pollution and Environmental Impact Analysis, American Meteorological Society, Boston, Massachusetts, pp. 59–111.

Briggs, G.A. 1984. "Plume Rise and Buoyancy Effects" Atmospheric Science and Power Production, DOE/TIC-27601, U.S. Department of Energy, Washington, D. C., pp. 327–366.

Brown, K.J. 1991. *Rocky Flats 1990-91 Winter Validation Tracer Study.* Report AG91-19, North American Weather Consultants, Salt Lake City, Utah.

Carhart, R.A., A. J. Policastro, M. Wastag, and L. Coke 1989. "Evaluation of Eight Short-Term Long-Range Transport Models Using Field Data." *Atmospheric Environment* 23 (1): 85–105.

Code of Federal Regulations (CFR). 1996. Guidelines for Air Quality Models. 40 CFR Part 51, Appendix W, August 12, 1996.

ChemRisk. 1992. *Reconstruction of Historical Rocky Flats Operations & identification of Release Points*. Project Task 3&4 for Phase I. Prepared by ChemRisk for the Colorado Department of Public Health and Environment. ChemRisk, A division of McLaren/Hart, 1135 Atlantic Avenue, Alameda, California 94501. March.

ChemRisk. 1994a. *Estimating Historical Emissions from Rocky Flats 1952-1989.* Project Task 5 for Phase I. Prepared by ChemRisk for the Colorado Department of Public Health and Environment. ChemRisk, A division of McLaren/Hart, 1135 Atlantic Avenue, Alameda, California 94501. March.

ChemRisk. 1994b. *Exposure Pathway Identification and Transport Modeling*. Project Task 6 for Phase I. Prepared by ChemRisk for the Colorado Department of Public Health and Environment, Denver, Colorado. ChemRisk, A division of McLaren/Hart, 1135 Atlantic Avenue, Alameda, California 94501. May.

ChemRisk. 1994c. *Dose Assessment for Historical Contaminant Releases from Rocky Flats.* Project Task 8 for Phase I. Prepared by ChemRisk for the Colorado Department of Public Health and Environment. ChemRisk, A division of McLaren/Hart, 1135 Atlantic Avenue, Alameda, California 94501. September.

Crow, L.W. 1974. *Characteristic Airflow Patterns near Rocky Flats Plant and Their Relationship to Metropolitan Denver*. LWC-143. Report prepared for Dow Chemical USA, Rocky Flats Division, December.

Decisioneering Inc. 1996. Crystal Ball Forecasting and Risk Analysis Software Version 4.0, Boulder Colorado.

DOE (U.S. Department of Energy). 1980. *Final Environmental Impact Statement, Rocky Flats Plant.* DOE/EIS-0064. April.

DOE. 1995. *Rocky Flats Environmental Technology Site Historical Data Summary*. AV-R--93-08-200. February.

EPA (U.S. Environmental Protection Agency). 1985. *Guideline for Determination of Good Engineering Practice Stack Height*. (Technical Support Document for the Stack Height Regulations), Revised. EPA-450/4-80-023R. Research Triangle Park, North Caroloina.

EPA. 1987. *On-Site Meteorological Program Guidance for Regulatory Modeling Applications*. EPA-450/4–87–013, Research Triangle Park, North Carolina.

EPA. 1992. *User's Guide for the Industrial Source Complex (ISC) Dispersion Models Vol. 1, User's Instructions*. EPA-450/4–92–008a. Research Triangle Park, North Carolina.

Finley, B., D. Proctor, P. Scott, N. Harrington, D. Paustenbach, and P. Price. 1994. "Recommended Distributions for Exposure Factors Frequently Used in Health Risk Assessment." *Risk Analysis* 14 (4): 533–553.

Genikhovich, E.L. and F.A. Schiermeier. 1995. "Comparison of United States and Russian Complex Terrain Diffusion Models Developed for Regulatory Applications." *Atmospheric Environment* 29 (17): 2375–2385.

Gifford, F.A. 1961. "Use of Routine Meteorological Observations for Estimating Atmospheric Dispersion." *Nuclear Safety* 2 (4): 47–51.

Gifford, F.A. 1983. "Atmospheric Diffusion in the Mesoscale Range: Evidence of Recent Plume Width Observations." Sixth Symposium on Turbulence and Diffusion, American Meteorological Society. Boston, Massachusetts.

Golden Software Inc. 1996. Surfer for Windows; Contouring and 3D Surface Mapping Software, Version 6. Golden Software Inc., Golden Colorado.

Grogan, H.A., W.K. Sinclair, and P.G. Voillequé. 1999. *Assessing Risks of Exposure to Plutonium.* 5-CDPHE-RFP-1998-FINAL(Rev.1). *Radiological Assessments Corporation*, Neeses, South Carolina. August.

HAP (Health Advisory Panel). 1993. *Health Advisory Panel's Report to Colorado Citizens on the Phase I Study of the State of Colorado's Health Studies on Rocky Flats.* Colorado Department of Public Health and Environment, Denver, Colorado.

Hammer, R.J. 1984. *An Analysis of Resuspension Source Area Impacts at Rocky Flats Surveillance Air Samplers S-7 and S-8 for Periods: July 25, 1983 – August 25, 1983 and September 8, 1983 – October 4, 1983.* Report RFP-3647. Rockwell International, Rocky Flats Plant, Golden Colorado.

Hardy, E.P. 1972. *Health and Safety Laboratory Fallout Program Quarterly Summary Report, December 1, 1971 – March 1, 1972*. HASL-249, Health and Safety Laboratory, U.S. Atomic Energy Commission, NY, NY.

Harper, F.T., S.C. Hora, M.L. Young, L.A. Miller, C.H. Lui, M.D. McKay, J.C. Helton, L.H.J. Goossens, R.M. Cooke, J. Pasler-Sauer, B. Kraan, and J.A. Jones. 1995. *Probability Accident Consequence Uncertainty Analysis, Dispersion and Deposition Uncertainty Assessment.* NUREG/CR-6244, U.S. Nuclear Regulatory Commission. Washington, D.C.

Hicks, B.B., K.S. Rao, R.J. Dobosy, R.P. Hosker, J.A. Herwehe, and W.R. Pendergrass. 1989. *TRIAD: A Puff-Trajectory Model for Reactive Gas Dispersion with Application to UF_6 Releases to the Atmosphere.* ERL ARL-168, National Oceanic and Atmospheric Administration, Air Resources Laboratory. Silver Springs, Maryland.

Hodgin, C.R. 1984. "Receptor-Based Techniques for Determining Impacts of Wind-Resuspended Particulates" In *HS&E Environmental Sciences Semiannual Progress Report for 1982 January through July*. Report RFP-3650. Rockwell International, Rocky Flats Plant, Golden, Colorado.

Hodgin, C.R. 1991. *Terrain-Responsive Atmospheric Code (TRAC) Transport and Diffusion: Features and Software Overview*. Report RFP-4516, EG&G Rocky Flats. Golden, Colorado.

ICRP (International Commission on Radiological Protection). 1995. *Age-Dependent Doses to Members of the Public from Intake of Radionuclides: Part 4, Inhalation Dose Coefficients*. ICRP Publication 71. Ann. ICRP 25, Nos 3 & 4. Pergamon Press, Oxford.

Killough, G.G., M.J. Case, K.R. Meyer, R.E. Moore, S.K. Rope, D.W. Schmidt, B. Shleien, W.K. Sinclair, P.G. Voillequé, and J.E. Till. 1998. *Task 6: Radiation Doses and Risk to Residents from FMPC Operations from 1951–1988*. Volume II, Appendices. 1-CDC-Fernald-1998-FINAL (Vol. II). *Radiological Assessments Corporation*. Neeses, South Carolina. September.

Layton, D.W. 1993. "Metabolically Consistent Breathing Rates for use in Dose Assessment." *Health Physics* 64 (1): 23–36.

Meyer, H.R., S.K. Rope, T.F. Winsor, P.G. Voillequé, K.M. Meyer, L.A. Stetar, J.E. Till, and J.M. Weber. 1996. *Task 2: The Rocky Flats Plant 903 Area Characterization.* RAC Report No. 2-CDPHE-RFP-1996-FINAL. *Radiological Assessments Corporation*, Neeses, South Carolina.

Miller, C.W. and L.M. Hively. 1987. "A Review of Validation Studies for the Gaussian Plume Atmospheric Dispersion Model." *Nuclear Safety* 28 (4): 522–531.

Miller, C.W., F.O. Hoffman, and D.L. Shaeffer. 1978. "The Importance of Variations in the Deposition Velocity Assumed for the Assessment of Airborne Radionuclide Releases." *Health Physics* 34: 730–734.

NCRP (National Council on Radiological Protection and Measurement). 1991. Some Aspects of Strontium Radiobiology. NCRP Report No. 110. National Council on Radiological Protection and Measurement, Bethesda, Maryland.

Pasquill, F. 1961. "The Estimation of the Dispersion of Windborne Material." *The Meteorological Magazine* 90: 33–49.

Petersen, W.B. and L.G. Lavdas. 1986. *INPUFF 2.0 - A Multiple Source Gaussian Puff Dispersion Algorithm: User's Guide*. EPA-600/8-86/024. Atmospheric Sciences Research Laboratory, U.S. Environmental Protection Agency. Research Triangle Park, North Carolina.

Press, W.H., S.A. Teukolsky, W.T. Vetterling, and B.P. Flannery, 1992. *Numerical Recipes The Art of Scientific Computing.* New York, New York: Cambridge University Press.

Ramsdell, J.V. Jr. 1990. "Diffusion in Building Wakes for Ground-Level Releases." *Atmospheric Environment* 24B (3): 337–388.

Ramsdell, J.V. Jr., C.A. Simonen, and K.W. Burk. 1994. *Regional Atmospheric Transport Code for Hanford Emission Tracking (RATCHET).* PNWD-2224 HEDR. Battelle Pacific Northwest Laboratories. Richland, Washington.

Robertson, E. and P.J. Barry. 1989. "The Validity of a Gaussian Plume Model When Applied to Elevated Releases at a Site on the Canadian Shield." *Atmospheric Environment* 23 (2): 351–362.

Rope, S.K., K.R. Meyer, M.J. Case, H.A. Grogan, D.W. Schmidt, M. Dreicer, T.F. Winsor, and J.E. Till. 1999. *Evaluation of Environmental Data for Historical Public Exposures Studies on Rocky Flats.* RAC Report No. 1-CDPHE-RFP-1997-Final(Rev.1). *Radiological Assessments Corporation*. Neeses, South Carolina. August.

Rood, A.S. 1999. *Rocky Flats Dose Reconstruction Project, Phase II: Performance Evaluation of Atmospheric Transport Models.* RAC Report No. 3-CDPHE-RFP-1996-FINAL(Rev.1). *Radiological Assessments Corporation*. Neeses, South Carolina. August.

Rood, A.S. and H.A. Grogan. 1999. *Comprehensive Assessment of Exposure and Lifetime Cancer Incidence Risk from Plutonium Released from the Rocky Flats Plant, 1953–1989.* RAC Report No. 13-CDPHE-RFP-1999-FINAL. *Radiological Assessments Corporation.* Neeses, South Carolina. August.

Roy, M. and C. Courtay. 1991. "Daily Activities and Breathing Parameters for Use in Respiratory Tract Dosimetry." *Radiation Protection Dosimetry* 35 (3): 179–186.

Seinfeld, J.H. 1986. *Atmospheric Chemistry and Physics of Air Pollution*. New York: John Wiley and Sons.

Simpson, D., D.A. Perrin, J.E. Varey, and M.L. Williams. 1990. "Dispersion Modeling of Nitrogen Oxides in the United Kingdom." *Atmospheric Environment* 24 (7): 1713–1733.

Slinn, W.G.N. 1984. "Precipitation Scavenging." In *Atmospheric Science and Power Production*. Edited by D. Randerson. DOE/TIC-27601. U.S. Department of Energy. Washington, D.C. 466–532.

Start, G.E., N.F. Hukari, J.F. Sagendorf, J.H. Cate, and C.R. Dickson. 1980. *ECOR Building Wake Effects on Atmospheric Diffusion.* ERL ARL-91 National Oceanic and Atmospheric Administration, Silver Spring, Maryland, November.

Stull, R.B. 1988. *An Introduction to Boundary Layer Meteorology*. Dordrecht, Netherlands: Kluwer Academic Publishers.

Turner, D.B. 1964. "A Diffusion model for an Urban Area." *Journal of Applied Meteorology* 3 (1): 83–91.

Voillequé, P.G. 1999. *Review of Routine Releases of Plutonium in Airborne Effluents at Rocky Flats.* RAC Report No. 6-CDPHE-RFP-1998-FINAL. *Radiological Assessments Corporation*. Neeses, South Carolina. August.

Whicker, F.W. and V. Schultz. 1982. *Radioecology: Nuclear Energy and the Environment*. Boca Raton, Florida: CRC Press Inc.

Zilitinkevich, S.S. 1972. "On the Determination of the Height of the Ekman Boundary Layer." *Boundary-Layer Meteorology* 3 (2): 141–145.